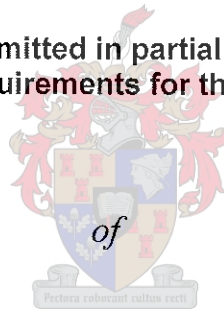# Effect of lime additions and bulk chromium content on chromium deportment in smelter matte-slag systems

By

Rudolph C. du Preez

**Thesis submitted in partial fulfillment
of the requirements for the Degree**

of

MASTER OF SCIENCE IN ENGINEERING
(CHEMICAL ENGINEERING)

in the Department of Process Engineering
at the University of Stellenbosch

Supervised by

**Prof. G. Akdogan
Prof. J. Eksteen
Mr. G. Georgalli**

STELLENBOSCH
DECEMBER 2009

Declaration

I, the undersigned, hereby declare that the work contained in this thesis is my own original work and that I have not previously, in its entirety or in part, submitted it at any university for a degree.

....
Signature

29-Feb-2010
....
Date

Synopsis

More mining houses are turning their attention to the processing of ore mined from the UG2 reef. This is mainly due to the depletion of the Merensky reef or the low availability of ore from the Platreef. With the higher UG2 ore concentration in the process feed, companies experience more problems with the processing of the ore due to its high chrome content. Although there are various possible solutions to the problems experienced in the processing of UG2 ore, very little of thise solutions are actually implemented in the industry.

When smelting chrome-bearing ore, the chrome can go to any of three phases: matte phase, spinel phase or glass phase. If it reports to the furnace matte phase it can lead to problems in the down stream processing. When chrome forms part of the spinel phase it forms a solid, refractory-like material which, to an extent, is an unwanted material inside the furnace. Lastly the chrome can report to the glass phase (liquid phase) which is the more desireable phase to which chrome should report to since it will have little or no impact on downstream processing.

There were four main objectives for this research project namely to conduct a literature review to understand the problem of chrome in the smelting process, to do an experimental simulation of a matte and slag phase in one crucible, to interpret the experimental results and compare the experimental results to thermodynamic predictions obtained using FactSage^{TM}.

From literature the following aspects were found to be important:

Silica structures

Research has shown that silica incorporates different metal ions into its structures. When the metal ions are incorporated into the silica structures they are seen as part of the glass phase. By incorporating cations such as chromium into the silica structure the structure is able to maintain its neutral electrical charge.

Basicity of slag

Oxides once melted will either donate or accept oxide ions. The group of oxides that are in excess will determine whether that specific slag is acidic or non acidic. This is important to our study since the basicity can determine the stability of the spinel phase.

<u>Partial pressures</u>

The partial pressure of the system is important since it forms part of the equilibrium constant calculations - meaning that partial pressures determine the stability of certain species. Currently different arguments exist as to how the sulphur pressure inside a molten bath is maintained. What is important, however, is that for the system in this research project a log oxygen partial pressure of -8 and a log sulphur partial pressure of -3.5 was chosen. These values were based on previous research done on PGM and copper smelting processes.

<u>Chrome deportment</u>

Previous research on chrome deportment shows a relationship between temperature and the amount of chromium dissolving into the glass phase as well as an increased chromium(II)oxide solubility (when compared to chromium(III)oxide) in a silicate melt. Regarding slag chemistry and chrome deportment very little work has been published for the system found in the PGM industry but it is mentioned that by adjusting certain slag additives (alumina, lime and silica) the chrome deportment can be manipulated.

The scope of this project was to investigate the effect of chromium, lime and silica on chrome deportment. More specifically, the effect of lime. The reason being that lime was originally added as 10%wt of the feed stream in the processing of Merensky ore to act as a fluxing agent. With the new furnace design and higher power densities the slag are maintained at $200^{o}C$ to $350^{o}C$ higher than when Merensky ore was smelted. With these higher slag temperatures fluxing agents will play a smaller role meaning that lime additions become less important. Literature studies also showed that additional lime in a slag system can stabilize the spinel structure (which is an unwanted phase). Removing lime would be advantageous out of a chrome presepective as well as an economic point of view.

The research was conducted in three sections namely the determination of the time required for this particular system to reach equilibrium, the investigation of different additives on chrome deportment using a controlled atmosphere and synthetic slags and, lastly, a comparison of the experimental results obtained to thermodynamic predictions.

For the equilibration studies reaction time periods of 4,7,11 and 16 hours were used. From the results it was found that the alumina crucible dissolved into the glass phase continually. This indicated that equilibrium was not reached. However, a reaction time, rather than an equilibrium time, was chosen where the species and phases had enough time to react. This was based on literature, on observations of species diffusing between the matte and slag phase as well as on two-point analysis (diffusion gradients). A reaction time of nine hours was chosen.

With the reaction time fixed, the effect of different slag additives on chrome deportment was investigated. For the addition of chrome it was seen that an 1.5%wt increase in the starting material increased the chrome content of the slag phase by 0.025%wt. For the same increase in chromium in the starting materials the chrome content of the spinel phase increased by 2.1% indicating that chromium has a tendency to report to the spinel phase. The increase in chromium had a minor effect on the chrome content of the matte phase, however, since the chrome content only increased from 0.025%wt to 0.028%wt.

Plotting the results showed that increasing the lime in the starting material decreases the chromium content in the glass phase. For the 39%wt silica system the chromium content in the glass phase decreased from 0.75%wt to 0.46%wt for an increase in the lime content from 1.7%wt to 7.3%wt. The same trend was seen for the 33%wt silica system. For the spinel phase an increase of 1.27%wt was seen when the lime content of the starting materials was increased from 1.7%wt to 10.1%wt for a 33%wt silica system. The same increase in lime increased the chrome content of the matte phase from 0.03%wt to 0.06%wt for a 33%wt silica system.

Silica also proved to affect chrome deportment. Increasing the silica content of the starting materials from 25%wt to 39%wt increased the amount of chromium in the glass phase from 0%wt to 0.46%wt for a 10%wt lime system. The same effect is seen for a lower lime content except that more chromium were incorporated into the silica structure. A silica increase from 32.4%wt to 39%wt resulted in a chromium decrease from 5.2%wt to 0% in the spinel phase for a 10%wt lime system. The same trend was seen for the 1.5%wt lime system. An increase in the silica levels lead to an increase in the chrome level of the matte phase. When silica is increased from 32%wt to 39%wt the chrome content of the matte phase increased from 0.06%wt to 0.07%wt.

The last part of the research project entailed the comparison of the trends observed with the experimental results to trends obtained from thermodynamic predictions. FactSage^{TM} is a program that uses model equations to predict the Gibbs free energies for different phases. The program is therefore also able to predict the amount of different phases present at equilibrium. This is called thermodynamic "optimization".

In section 6 trends that were observed from FactSage^{TM} results are compared to the trends found in the experimental results. It is important to note that it is only trends that are evaluated and not actual values since FactSage^{TM} calculations are for a system that is at equilibrium and (as explained above) this system is not at complete equilibrium. The comparison however was good. Several trends found in the experimental results were confirmed by the results from FactSage^{TM}. These included the relationships of chromium fed versus chromium spinel, lime fed versus chromium spinel, lime fed versus chromium in glass, silica fed versus chromium in glass, silica fed versus chromium in spinel and silica fed versus chromium in matte.

To conclude, slag additions can be used to manipulate chrome deportment to an extent. Secondly, FactSage^{TM} can be used for thermodynamic predictions but a proper understanding as well as some form of validation of the specific system investigated is still needed.

Due to time constraints and the difficulty of experimentally simulating this multi-phase system in the lab, only a few parameters were investigated. In order to obtain a more complete understanding of the system the effect of partial pressures and temperature should also be investigated.

Contents

Chapter 1

Introduction

1.1 Rationale

South Africa is the world's largest producer of platinum group metals (also known as PGM'S) and its ore body makes out about 80% of the world's reserves [1]. The ore body is associated with three different reefs. These reefs are called the Platreef, Merensky reef and the UG2 reef and together they are known as the Bushveld complex. Early tendencies in the platinum industries were to process mostly Merensky or Platreef material since these materials are easier to process [2] [3]. However, due to the demand mining houses are starting to deplete their sallow Merensky reserves and is now turning to the processing of material mined from the UG2 reef [3].

The UG2 reef has a higher chrome content than the Merensky and the Platreef. This higher chrome content leads to several problems in the platinum industry. Concentrators must now not only control their process for PGM recovery but must also control the amount of chrome that is entrained in their overflow. Even with the concentrators controlling their chrome dispatch it is still necessary to make adjustments to the smelting process due to the higher chromium in the concentrate compared to when the Merensky reef or Platreef were processed. Without these adjustments the high chrome content of the UG2 reef could lead to the following main problems during furnace operation:

1. The formation of solids. Chromium react with iron to form a solid material called spinel. It is suspected that these solids increase the density and viscosity of the glass phase [3].

2. When these solids (spinels) settle they can lead to the formation of build-up inside a furnace [1].

3. A higher chrome content in the furnace matte phase. This is problematic for converter operation [4].

Other problems are listed in section 2.6.2. Various solutions to these problems have been identified. Some examples include: the use of high intensity furnaces where higher power densities are used to try and keep the spinel in suspension, selective solidification of oxides which at this stage is only an proposal and is not yet practiced or tested, alternative furnace setup/technologies which include the desulphurization of the concentrate and DC arc technology.

Another possible solution, and the one this research focuses on, is the adjustment of the slag chemistry inside furnaces to force more of the chromium into the "harmless" glass phase leading to less chromium reporting to the matte phase or the unwanted spinel phase. The glass phase has the potential to incorporate the chromium ion as part of the silica structure. The capacity or amount of chromium will depend on various factors including the basicity of the slag as well the partial pressure of the melted material. The effect of these factors on chrome deportment are still not properly understood and literature on this topic is limited. However, if studies prove that slag manipulation could dissolve more chromium into the glass phase it would be one of the easiest solutions to implement.

1.2   Scope

The oxide components in the concentrate include lime, magnesia, alumina, iron and silica. For this project only different additions of lime, silica and chrome will be investigated. However, for Lonmin specific focus will be on the effect of lime on chrome deportment. The reason being that lime was originally added as 10%wt of the feed stream in the processing of Merensky ore to act as a fluxing agent. With the new furnace design and higher power densities the slag are maintained at 200°C to 350°C higher than when Merensky ore was smelted. With these higher slag temperatures fluxing agents will play a smaller role meaning that lime additions becomes less important. Literature studies also showed that additional lime in a slag system can stabilize the spinel structure (which is an unwanted phase). Removing lime would therefore be advantageous out of a slag chemistry point of view as well as an economic point of view.

The scope of this project is to establish from the literature what parameters affect chrome deportment between different phases and to then experimentally investigate chrome deportment using synthetic slags that are based on slag systems found in the industry. The aims of this project were to:

1. Successfully simulate a matte/slag phase inside a tube furnace using an alumina crucible and a controlled atmosphere.

2. Determine the reaction time that is required to come as close to equilibrium as possible.

3. Determine the optimum amount of lime and chrome fed to the furnace.

4. Investigate whether basicity has an effect on chrome deportment.

5. Compare trends obtained from experimental results to thermodynamic predictions obtained from FactSage^{TM}.

Chapter 2

Theoretical background

2.1   The bushveld complex

South Africa's platinum ore makes up about 80% of the world's reserves. The platinum ore body, or Bushveld complex, consists out of three layers namely the Merensky reef, the Platreef and the UG2 reef. Depending on the location, the Merensky reef can be found at a depth of 130m [5]. The platinum group metals in the Merensky- and Plat reef are associated with base metal sulphides [1]. The base metal sulphides consist of :

1. Pyrrhotite and pyrite (Iron sulphides)

2. Pentlandite (Iron nickel sulphides)

3. Chalcopyrite (Copper iron sulphides).

The base metal sulphides are embedded alongside pyroxene with interstitial plagioclase [5]. Orthopyroxene [$(Fe,Mg)SiO_3$] and plagioclase [$CaAl_2Si_2O_8$] are silicate compounds which are seen only as gangue [1].

The Platreef is situated on the northern limb of the Bushveld complex and has a similar composition to the Merensky reef but is of less importance to this project since Lonmin is only mining Merensky and UG2 ore. This leaves the UG2 reef that runs under the Merensky reef. With the depletion of the Merensky reef, companies will turn more towards the UG2 reef as a source of platinum group metals [3].

The UG2 reef is known to be a chromite layer embedded by plagioclase and orthopyroxene [1]. Table 2.1 shows the different compositions for the Merensky reef and UG2 reef.

Table 2.1 was adopted from Nell 2004.

Table 2.1: The average composition of the Merensky-and UG2 platinum concentrate received from concentrators

	Al_2O_3	Cr_2O_3	Cu+Ni	Fe	MgO	S	SiO_2	PGM
Units	Mass %	Mass %	Mass %	Mass %	Mass %	Mass %	Mass %	PPM
Merensky	1.8	0.4	5	18	18	9	41	130
UG2	3.6	2.8	3.3	12	21	4.1	47	340

By comparing values in Table 2.1 it can be seen that the UG2 reef may contain more platinum group metals than the Merensky reef. This is also mentioned by another author [1].

Table 2.1 also shows the large difference in the chrome content between the Merensky reef and UG2 reef. The high chrome content is one of the major reasons why companies would prefer mining the Merensky reef. The Merensky reef was the main source of platinum in South Africa up until 1970 due to the problems that developed with the additional chrome in the UG2 reef. With the improvement of metallurgical technology, mining companies started to feed a blend of UG2 and Merensky ore into their processes. Today this approach is common practice [2].

2.2 The platinum production process

The platinum production process can be divided into three stages namely: the mining stage, the smelting stage and the refining stage.

The Mining and Extraction Stage

Platinum ore is either mined from an open pit source or from underground reserves. The ore obtained from the shafts are sent to the concentrator plants. At the concentrators the ore gets crushed and milled. After milling the slurry it is sent to the primary flotation section which consist of stages of rougher cells (which recover any material that floats) and stages of cleaner cells (which selectively recover base metals through correct chemical dosing and air intake). A secondary milling and floatation section is used as a scavenger circuit to collect some of the PGM's that did not float in the primary circuit. The concentrate produced from the final primary cleaners and final secondary cleaners are combined and sent to the smelter for further processing [6].

Smelting Section

From the concentrators the material (concentrate still as a slurry) is transported to the processing section. Here the slurry is blended with slurries from different concentrators in order to maintain the chrome level that would be fed

to the furnaces. The blended slurry is pressed (filtered) and then dried using a flash dryer before stored or sent to the furnaces.

The Six-In-Line furnace is the most widely used furnace system [7]. Power input to a six in line furnace ranges between 10MW to 75MW. Higher power inputs were made possible with copper cooling systems fitted to these furnaces enabling the furnace to form a protective freeze lining. The power flux for a Six-In-Line furnace is in the order of 90-165kW/m^2 which is lower than the power flux achieved using three electrodes in a triangular setup (320kW/m^2 at 28MVA) [1]. The higher power flux of the three electrode setup is beneficial when feeding chromium bearing ore such as UG2 because it will help to keep the solid material in suspension. This is one of the reasons why some companies started using the three electrode system [7].

The purpose of the furnace is to take the material into a molten state. In the molten state two layers starts to form. The first, or top, layer is called a slag layer and contains mostly iron-oxides and silicates. It is in this top layer that droplets, containing sulphides, starts to form. As these droplets grow in size they will separate from the slag phase due to the difference in their densities [1]. This separation process is influenced by viscosity which is controlled by adding fluxes to the furnace. The droplets from the slag layer will group and form the second, or bottom, layer called the matte layer. The matte usually consists of iron-copper-nickel sulphides and platinum group metals (PGM's) [1].

Barnes [3] as well as Jones [8] states that there is a third layer which forms in between the matte and slag layers. This layer forms due to the density of the slag layer approaching the density of the matte layer which occurs when the chromium content of the slag is increased.

From the furnace the matte, that is periodically tapped, is sent to the converter. In the converter air is blown through the molten material to oxidize iron and sulphur to form a new slag and matte system. Historically slag from the converter was recycled to the primary furnace but due to some advantages of not recycling, including the lowering of chromium spinel buildups, new trends such as a slag cleaning furnaces or a floatation system are used [9]. At Lonmin converter slag as well as furnace slag is milled floated and blended with the concentrate slurry.

<u>Base metal recovery and Refining stage</u>

From the converter the granulated matte is sent to the Base metal Recovery (BMR) where copper, nickel and sulphur are removed. The final product from the BMR is sent to Precious Metal Refinery (PMR) for refining. Refining is the last stage in producing platinum. In this stage all the base metals such as copper and nickel are removed from the PGM containing material. Electrolytic techniques, solvent extraction, distillation and ion exchange procedures are used to purify the PGM'S from gold and silver.

2.3   Slag chemistry

Most valuable minerals are located in a ore body containing a large amount of oxides [10]. This means that during the melting of minerals a by-product (called slag) will form. Slag consists of mostly oxides and some metals that was entrapped. This section discusses some of the chemistry observed inside these slags.

2.3.1   Silica structures

Platinum group metal recovery is associated with a silica-based slag. In furnace operation silica can associate itself with different metal ions to form silicate minerals such as pyroxenes. Since the compositions that will be studied in this project is rich in silicate it is likely that silicate minerals will form inside the system. The silicate structures are comprised of unit structures, or $(SiO_4)^{-4}$, and can be linked using different mechanisms[11]. The mechanisms are given below:

1. Without sharing oxygen ions. e.g. $(Mg)_2SiO_4$

2. The sharing of one oxygen ion. This structure will consist of a pair of unit cells $(SiO_4)^{-4}$ that are bonded to the cations ionically e.g. $Zn_4Si_2O_7$. $(OH)_2.H_2O$

3. The sharing of two oxygen ions. In this situation a infinite number of unit cells can link to form chains. These chains are then linked together by a cation e.g. $LiAl(SiO_3)_2$.

From the bonding mechanism mentioned above it can be seen that all the structures incorporates cations such as the chromium ion. The cations are necessary to keep the electrical charge of the compound neutral [11]. Figure 2.1 shows the polymerization of the silica unit structure.
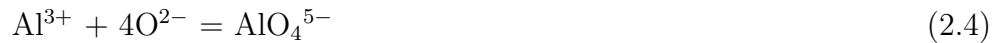
2.3.2   The basicity of slags

Oxides can be divided into two groups. The first group of oxides will accept oxide ions, O^{2-}, as in equation 2.1 and the second group would rather donate their oxide ions such (see equation 2.2). In between acidic and basic oxides there are neutral oxides such as Cr_2O_3, MgO, Al_2O_3 and Fe_2O_3. These compounds can take part in reactions like those expressed in equation 2.3 and equation 2.4. From these two equations it is evident that the state of some species are determined by the basicity of the slag, the amount of oxygen ions
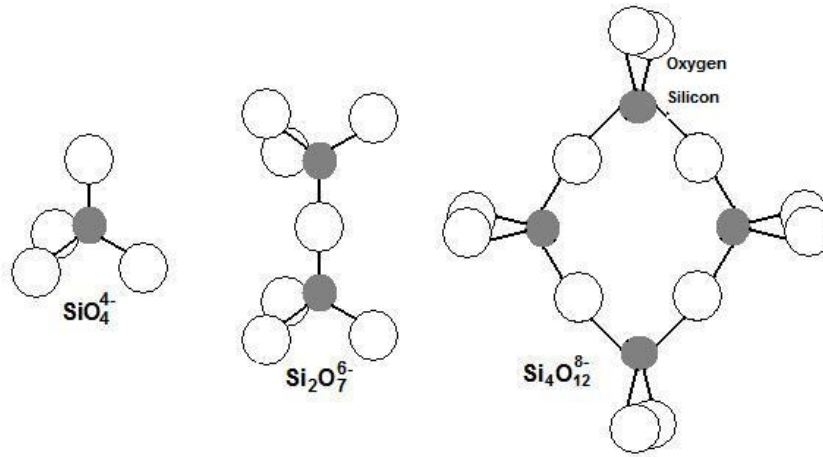
Figure 2.1: Crystalline silicates

in the slag, which in the case of this project are controlled by lime and silica additions [10].

$$SiO_2 + O^{2-} = SiO_4^{-4} \tag{2.1}$$

$$CaO = Ca^{2+} + O^{2-} \tag{2.2}$$

$$Al_2O_3 = 2Al^{3+} + 3O^{2-} \tag{2.3}$$

$$Al^{3+} + 4O^{2-} = AlO_4{}^{5-} \tag{2.4}$$

Basicity of slags are an arbitrary number calculated using the ratio between acidic and non acidic species. The species included in the calculation are based on the specific industry and their specific slag system. In this study basicity was calculated using the ratio of lime plus magnesia over silica. Basicity of slags are important to this study since a basic slag can attack a slag that is acidic and vice versa. The basicity of the slag in this study can therefore affect the formation of spinel, which is seen as a refractory material.

2.3.3 The oxygen and sulphur partial pressures

During the smelting process a gas atmosphere, with a certain oxygen and sulphur paritial pressure, is formed inside the furnace as a result of chemical reactions taking place. Nell [7] states that oxygen partial pressure is controlled by the QFM redox reaction (see equation 2.5).

$$3Fe_2SiO_4 + O_2 = 2Fe_3O_4 + 3SiO_2 \tag{2.5}$$
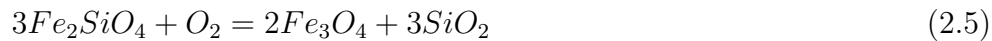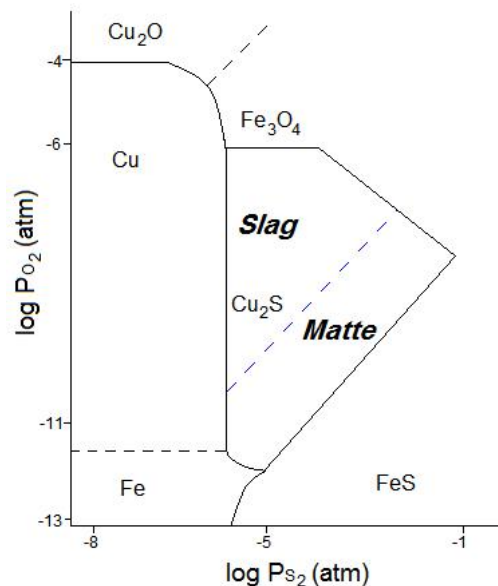
Figure 2.2: Sulphur-oxygen potential diagram for the Cu-Fe-O-S-SiO_2 at 1300^oC [13]

Equation 2.5 accounts for the oxygen partial pressure but doesn't indicate any interaction between the oxygen and sulphur pressure. Kho [12] describes this interaction with the following equation [12]:

$$FeS + \frac{1}{2}O_2(g) = FeO + \frac{1}{2}S_2 \tag{2.6}$$

Where the equilibrium constant is defined as:

$$K_{Fe} = (a_{FeO}/a_{FeS})(p_{S2}/p_{O2})^{\frac{1}{2}} \tag{2.7}$$

The measurement of the gas partial pressure inside the furnace is a daunting task due to the extreme nature of the smelting process. However, Mintek investigated the partitioning of gallium (Ga_2O_3) and tin (Sn^o) and found the log oxygen partial pressure to be in the order of -8 to -9 [7]. This is also confirmed by the sulphur-oxygen potential diagram given in figure 2.2. The sulphur-oxygen diagram is a simplified version from an article by Yazawa for a copper-iron-silica melt at 1300^oC [13]. From the diagram the matte phase is stable under log partial pressure of sulphur of -5 up to -1 depending on the oxygen partial pressure. However, the higher the sulphur partial pressure, the more oxidizing the conditions inside the furnace become. This relationship is also mentioned by Kress [14].

The oxygen- and sulphur partial pressures of a system are two very important properties since these two values will determine what oxides and sulfides
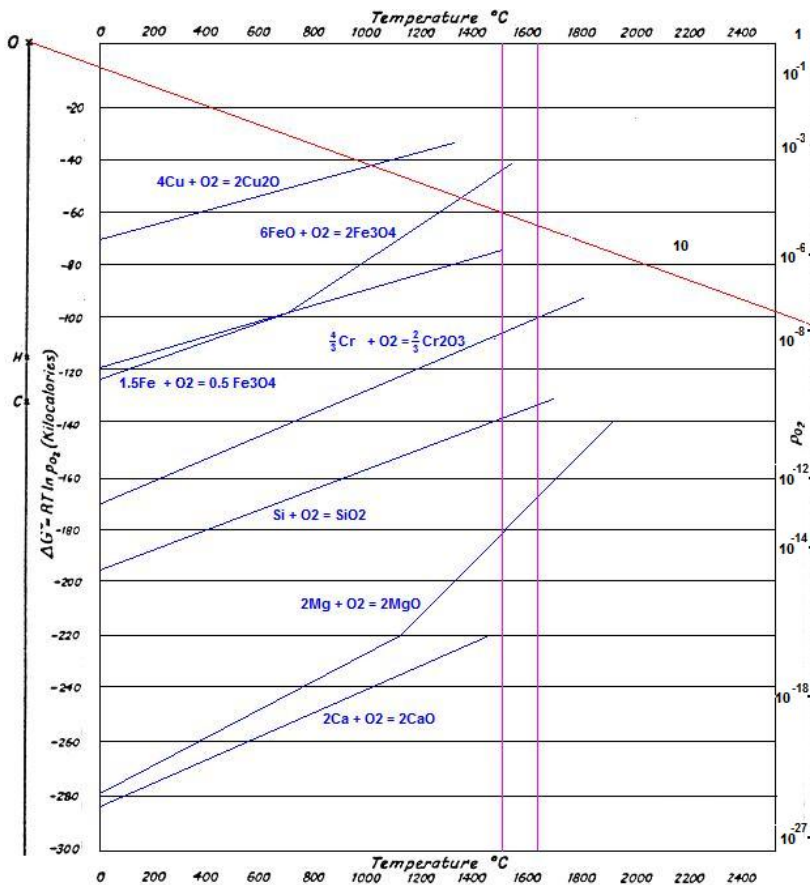
Figure 2.3: A simplified Ellingham Diagram

will form during the smelting process. The relationship between the partial pressure and the species that forms can be explained by thermodynamics. From thermodynamic principles the standard free energy of formation can be calculated using equation 2.8.

$$\Delta G_f^o = \text{-}R \cdot T \cdot \ln(K) \tag{2.8}$$

For the reaction described in equation 2.9 the equilibrium constant defined by equation 2.10. If you have a pure metal species the activities given by a will be equal to one. Thus, equation 2.8 can be rewritten into equation 2.11.

$$M + O_2(g) = MO_2 \tag{2.9}$$

$$K = \frac{a_{MO_2}}{a_m \cdot P_{O_2}} \tag{2.10}$$

$$\Delta G_f^o = R \cdot T \cdot ln(P_{O_2)} \tag{2.11}$$

Equation 2.11 defines the partial pressure of oxygen in terms of the formation energy of a metal oxide. The same procedure can be followed to define the formation energy of metal sulfides in terms of partial pressure of sulphur.

Ellingham was the first person to plot the standard Gibbs free energy of formation against the temperature and saw that the relationship between these two properties were mostly linear. This plot is called the Ellingham diagram. Richardson took the Ellingham diagram and added the effect of oxygen partial pressure on the formation of different oxides. Including the effect of partial pressure in the Ellingham diagram makes it easy to predict which oxides will be stable under a certain oxygen partial pressure and temperature. Figure 2.3 is a simplified Ellingham diagram for oxides. The same diagram can be drawn for sulfides and the sulphur partial pressure.

In figure 2.3 the red line anchors the oxygen partial pressure at which our system will operate and the two pink lines indicate the temperature band. From the figure it is evident that the partial pressure is to high for any metal oxides to be reduced. However, the figure indicates that there should be some equilibrium between iron(II)oxide and iron(III)oxide.

2.4 Previous research on phase equilibria systems relevant to this project

In this section equilibria systems and properties previously researched will be mentioned and discussed. The purpose of this section is to develop an understanding of these type of systems which will help in understanding the results of this project.

2.4.1 The matte phase

The matte phase also known, as a sulphide melt, is composed of sulphide-associated metals such as nickel, iron and copper. Due to the difference in density of the matte phase and the slag phase, separation inside the furnace will occur (matte which is more dense will settle to the bottom of the furnace). When attemping to maintain a sulphide melt it is neccesary to maintain the correct sulphide and oxygen partial pressures. In section 2.3.3 the conditions under which a matte and slag phase would coexist, were discussed. The sulphur and oxygen content of the sulphide melt are influanced by the gas partial pressures, base metal content of the slag and temperature.

Figure 2.4 illustrates that as the sulphur partial pressure increases the sulphur content of the matte increases as well. The figure also indicates that the effect of partial pressure on the sulphur content is influenced by temperature. For a log sulphur partial pressure of -3 a nickel based matte would have a
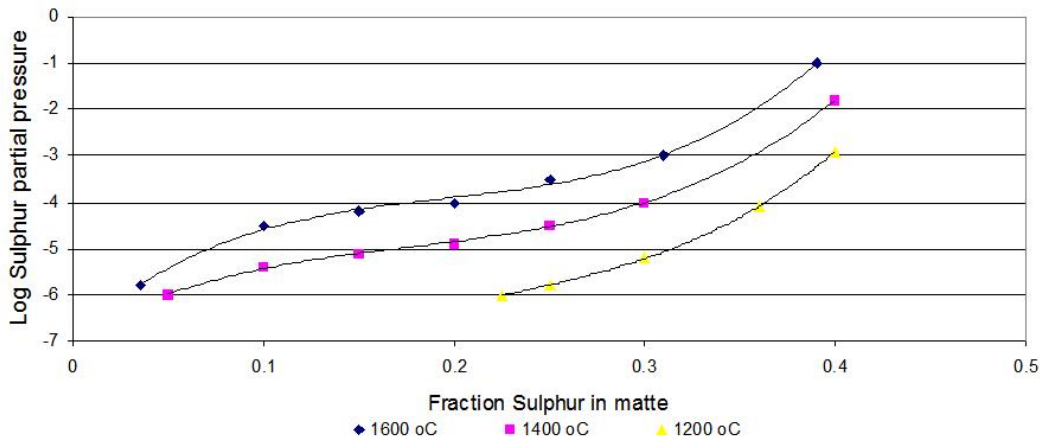
Figure 2.4: Sulphur partial pressure versus the sulphur content of a nickel sulphide matte [14]

sulphur content of 31%wt. For the same partial pressure but with a 200°C decrease in temperature, the sulphur content will increase by 5%wt.

Knowing the effect of sulpur partial pressure and temperature on the sulphur content it is neccesary to expand the investigation by studying a copper-iron-nickel matte with different iron ratios (refer to figure 2.5). The iron ratio R_{Fe} is defined as the amount of iron over the sum of iron, nickel and copper. In figure 2.5 it can be seen that similarly to figure 2.4, an increase in sulphur partial pressure will increase the weight percentage of sulphur in the matte phase. However, this figure also indicates that for the same sulphur potential a higher R_{Fe} makes the matte capable of accumalating more sulphur (for a log sulphur potential of -3 the sulphur content of the matte phase would increase with 6%). Figure 2.5 was adapted from a study by Wright , in his study he also investigated the effect of sulphur partial pressure on the distribution of copper, nickel and iron between an alloy phase and a matte phase [15]. The latter is discussed in section 2.4.2.

In the remainder of this section the individual sulfide components will be discussed.

The nickel-sulfide system

The nickel-sulfide phase diagram is given in Figure 2.6. The phase diagram shows that the nickel sulfide compounds that are stable at room temperature are NiS, Ni_3S_2 and Ni_7S_6. Upon heating the Ni_7S_6 will change into the Ni_3S_2 phase. A eutectic point exists at a temperature of 637°C and a composition of 33.4% sulphur. The liquidus temperature in the phase diagram ranges from 637°C to 1453°C depending on the sulphur composition.
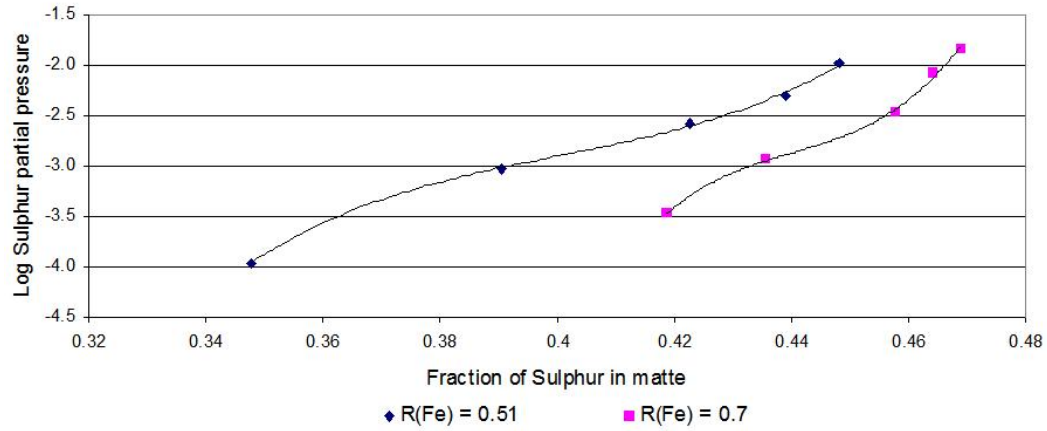
Figure 2.5: Sulphur partial pressure versus the sulphur content of a copper-iron-nickel sulphide matte at 1400°C [15]
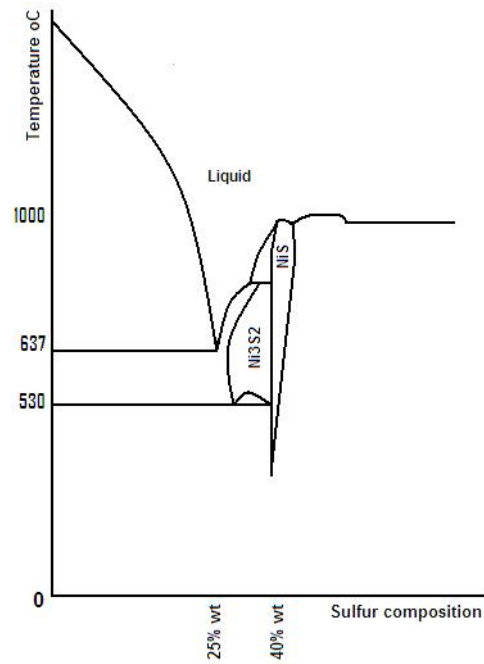
Figure 2.6: The nickel sulfide diagram. The original phase diagram was published in Smithells and Metals [16]
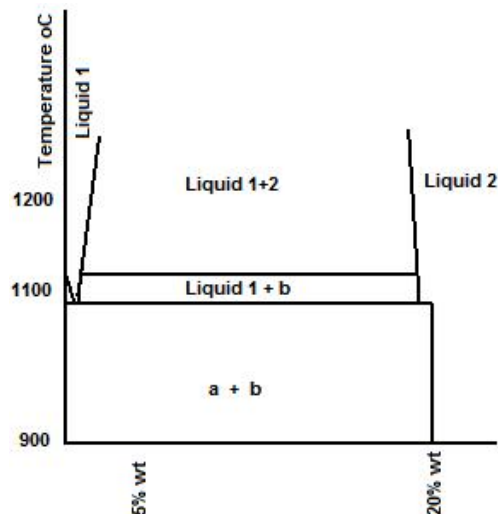
Figure 2.7: The copper sulfide diagram. The original phase diagram was published in Smithells and Metals [16]

The copper-sulfide system

Figure 2.7 represents the copper sulfide phase equilibria system. The phase diagram in figure 2.7 is only for a sulphur composition between 2%wt - 20%wt and a temperature range of 900°C to 1300°C. Observations that can be made from this phase diagram are that at a sulphur composition of 1.5%wt to 20%wt and a temperature above 1105°C there exists two immiscible liquids. The two liquids become miscible at a sulphur composition lower than 2%wt and above a sulphur composition of 19%wt. As the liquids cool down, below 1105°C and above 1067°C, the liquid goes into equilibrium with the beta phase. Upon further cooling, below 1067°C, all the liquid turns into a solid state.
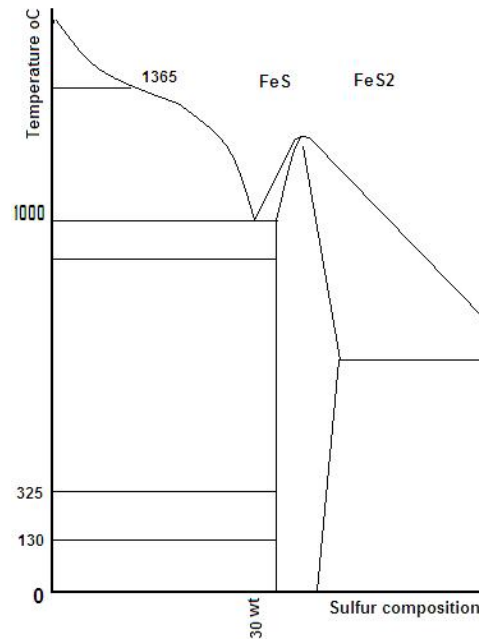
The iron-sulfide system

The phase diagram (see figure 2.8) illustrates that for an iron iron-sulfide system the liquidus phase stretches across the entire diagram. A monotectic reaction is seen at a sulphur composition of 12.5%wt and lower and at a temperature of 1365°C.

Another observation from the phase diagram is that at a sulphur composition of 30%wt and a temperature of 988°C an eutectic point is formed. The phase changes at temperatures lower than 1000°C will not be discussed since it is not applicable to this work.

2.4.2   The solubility of Cr_2O_3 into the glass phase

In an article by Nell it is explained that the solubility of chromium oxide into the slag phase is a function of three factors namely temperature, oxygen partial

Figure 2.8: The iron sulfide phase diagram. The original phase diagram was published in Smithells and Metals [16]

pressure and slag composition [7].

Temperature

Figure 2.9 indicates the relationship between the solubility of Cr_2O_3 in the slag phase and the temperature. The slag used to generate the data points for figure 2.9 contains 6.4%wt percent Al_2O_3, 10.4%wt percent FeO, 31%wt percent MgO, 6%wt percent lime and 45%wt percent silica. From the figure an increase in temperature from 1300^oC led to an increase in the solubility of chromium oxide in the slag phase. However, for a temperature increase of 200^oC the weight percentage of Cr_2O_3 in the slag phase only increased from 0.2%wt up to 0.6%wt.

Oxygen potential

The solubility of chromium oxide into the glass phase is also a function of the oxidation state of the chromium ion which, in turn is a function of the oxygen partial pressure of the system [17]. A general rule for base metals is that the lower the valance of the ion the more soluble the ion will be in liquid silicate [7].

In Neil Bartie's work this statement was proved to hold for chromium [18]. Bartie 2004 investigated log oxygen partial pressures between -10 atm and -04 atm and a bulk chromium oxide content ranging from 1.5%wt to 6.4%wt.
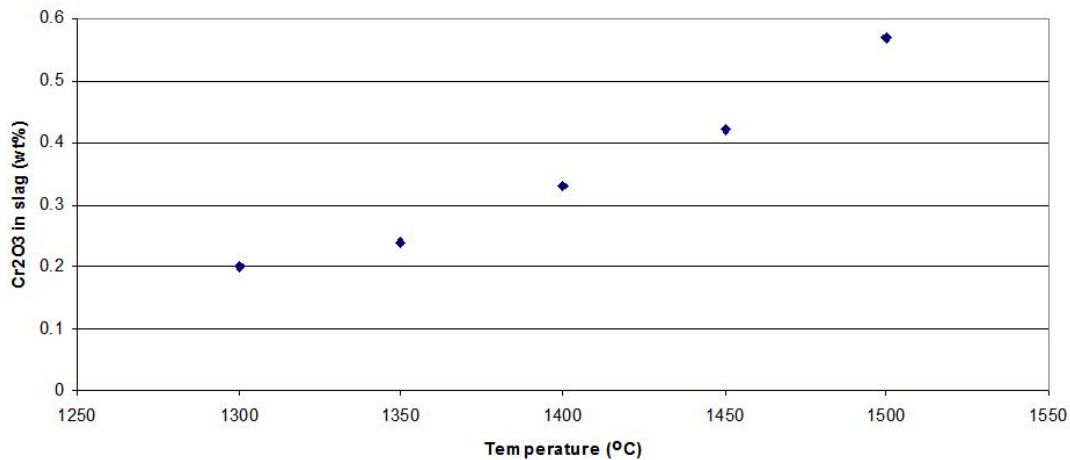
Figure 2.9: The effect of temperature on the solubility of chromium oxide into a slag phase [7]
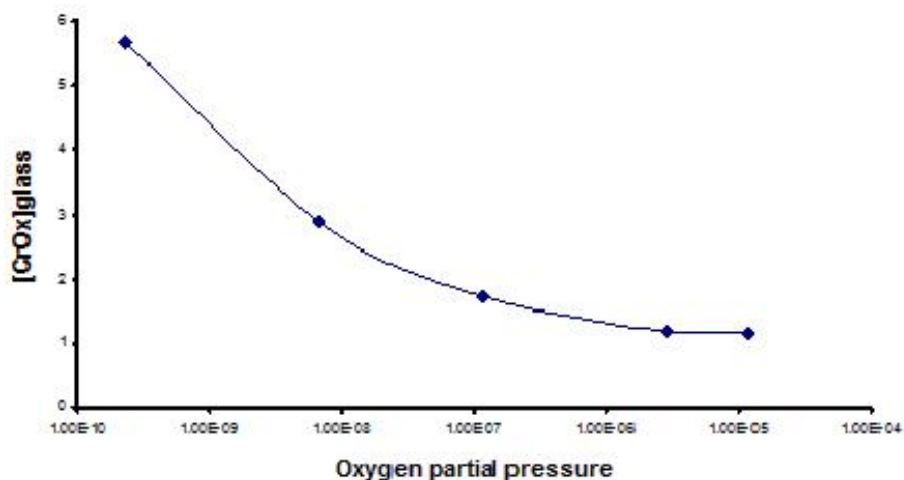

Figure 2.10: The effect of the partial pressure of oxygen to the solubility of Cr into the slag phase. The diagram was simplified from Neil Bartie

Figure 2.10 is a representation of his results. Figure 2.10 shows the amount of chromium oxide that dissolved into the slag phase ranges from 6%wt to 1%wt. This solubility of an chromium ion into the silica melt is illustrated in figure 2.11.

By comparing phase diagrams A and B, in figure 2.11, it is clear that the chromium(II)oxide is more soluble in a silica melt than chromium(III)oxide. In figure2.11, for the trivalent ion, the liquid region only starts at a temperature of 2300^oC except when the SiO_2 is near to a hundered percent, whereas in figure 2.11 B, the liquid region starts at a temperature of 1400^oC.
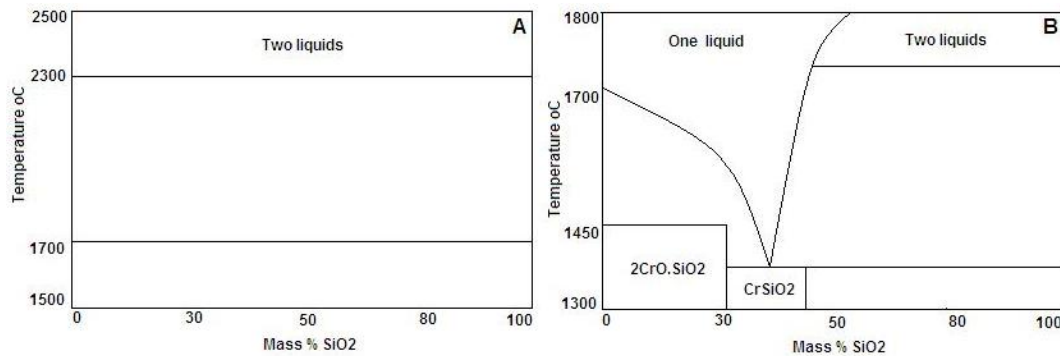
Figure 2.11: The chrome-silica system. In diagram A chromium is in a trivalent oxidation state and in diagram B in a divalent oxidation state [7].

Slag chemistry

The effect of slag chemistry on the solubility of chromium oxide is still relatively unknown but investigations showed that the solubility of chromium oxide is to an extent a function of basicity [7]. Figure 2.12 indicates that a decrease in basicity will cause a decrease in the amount of Cr_2O_3 that dissolves into the glass phase. The figure also indicates that the effect of basicity is less severe at a higher oxygen potential.

Investigation by Mintek on the slag additives and chromium oxide solubility did reveal the following trends. Only the trends, and not he actual values, of the results will be discussed to prevent the possibility of revealing any confidential information [19].

1. By increasing the amount of Al_2O_3 in the slag the amount of Cr_2O_3 in the glass phase will decrease.

2. An increasing amount of CaO will result in decreasing the amount of Cr_2O_3 in the glass phase.

3. An increasing amount of SiO_2 will result in increasing the amount of Cr_2O_3 in the glass phase.

2.4.3 The solubility of copper into an iron silicate slag

Kim worked on an iron silicate slag system at a temperature of 1250°C and an log oxygen partial pressure range of -12 to -6 atm. Kim studied the effect of additives on the copper solubility in slag [20]. The mass percentages of the additives that were investigated are given in Table 2.2.
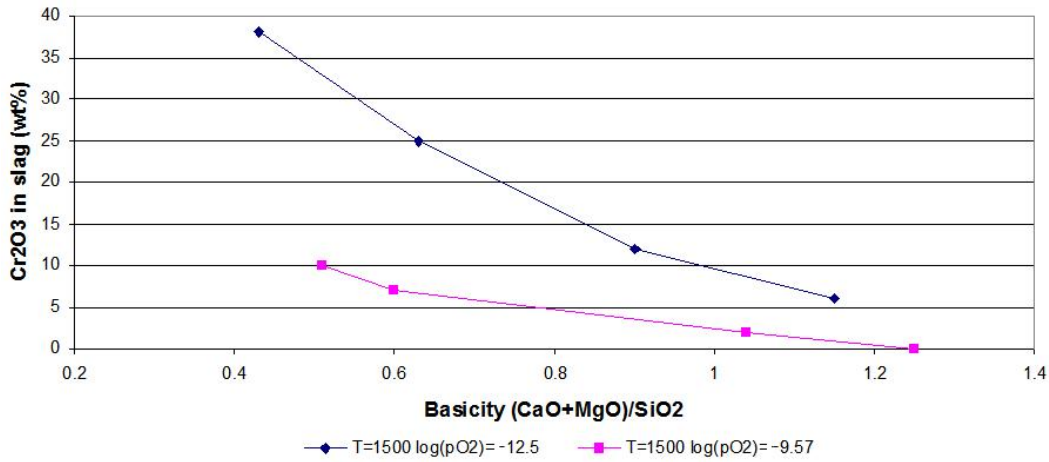
Figure 2.12: The effect of basicity on the solubility of chromium oxide into the liquid slag phase [7].

Table 2.2: The mass percentages used in the research conducted by Kim [20]

Species:	Min weigh percentage	Max weight percentage
CaO	4.4%	11.9%
Al$_2$O$_3$	4.4%	8.2%
MgO	4.4%	-

The results of the research showed that the copper solubility decreased with an increase in the amount of CaO, MgO and Al$_2$O$_3$ added to the slag. CaO lowered the copper solubility the most with a reduced effect for MgO and still lower for Al$_2$O$_3$ [20].

Kim also noted that the effect of additives on the copper solubility showed some relation to the size of the ions of the specific additives . It was determined that the Ca ion had a very similar radius to that of copper where as the radius for Al^{3+} was much smaller. This indicates that chromium would most likely also compete with other ions for a place in the silica structure.

2.4.4 The CaO-CrO-SiO$_2$ System

The CaO-CrO-Cr$_2$O$_3$-SiO$_2$ system in equilibrium with chrome was investigated by De Villiers [21]. He investigated the system under a log oxygen partial pressures of -10 atm and -13 atm. Table 2.3 reports the minimum and maximum weight percentages used in De Villiers research.

Table 2.3: The minimum and maximum weight percentages that were used in the research conducted by De Villiers [21]

Species:	Min weight percentage	Max weight percentage
CaO	2%	65%
SiO$_2$	1%	84%
CrO	7%	97%

Table 2.4: The phases present under severe reducing conditions De Villiers 1992 [21]

Temperature:	1340°C	1400°C	1450°C	1700°C	1780°C
Phase					
CaO					X
Ca$_3$SiO$_5$	X	X			X
CaCr$_2$O$_4$			X	X	X
CaCrSi$_4$O$_{10}$			X	X	
(Ca$_{0.6}$Cr$_{0.4}$)Cr$_2$O$_4$		X	X		

Table 2.5: The phases present under less reducing conditions De Villiers 1992 [21]

Temperature:	1430°C	1440°C	1454°C
Phase			
Cr$_2$O$_3$	X	X	X
Ca$_3$Si$_2$O$_7$		X	
CaSiO$_3$	X	X	
Ca$_2$SiO$_4$			X
Ca$_2$Si$_2$O$_7$	X		

De Villiers found that under extreme reducing conditions (in contact with metallic chrome) the Cr became more soluble, by replacing Ca, than in less reducing conditions. Table 2.4 shows the different invariant points and phases present in the more severe reducing conditions. Table 2.5 shows the phases present under the less reducing conditions. Comparing the two tables it is clear that in less reducing conditions the chromium ion did not replace the calcium ion.

2.4.5 The Cr$_2$O$_3$-FeO$_x$-SiO$_2$ System

Figure 2.13 illustrates the phase diagram for the Cr$_2$O$_3$-FeO$_x$-SiO$_2$ slag system. The phase diagram has been simplified from the Slag Atlas. The original equilibria research was conducted by Muan [22].
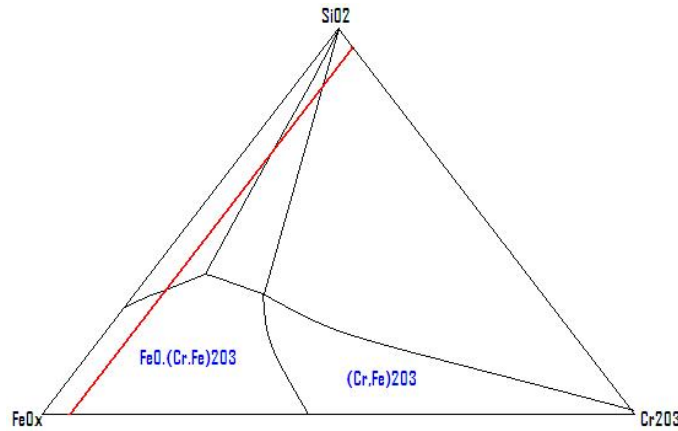
Figure 2.13: The Cr_2O_3-FeO_x-SiO_2 phase diagram. The original phase diagram was published in the Slag Atlas [23]

Figure2.13 illustrates that at a Cr_2O_3 composition of 10wt% and lower and at a FeO_x composition greater than 80%wt spinel formation will start to take place. From this figure it can also be seen that when the SiO_2 composition increases there are no spinel formation.

2.4.6   The CaO-SiO_2-FeO_x System

The CaO-SiO_2-FeO_x system is given in figure 2.14. The phase diagram has been simplified and only shows the compounds that are likely to form in the system studied in this project. The original diagram was created by Osbourne and Muan 1960. The experimental results of Bowen 1933 were used.

In figure 2.14 there are three crystalline structures that forms at a CaO composition of 5wt% and less. These structures are Wustite [(Fe,Ca)O], Olivine [2(Fe,Ca)O.SiO_2] and Cristobalite [SiO_2].

The liquidus temperature, in the Wustite area on figure 2.14, ranges between 1200^oC to 1283^oC and increases as the amount of iron oxide increases. The liquidus temperature for the olivine area ranges between 1105^oC to 1130^oC and increases with an increase in lime. The liquidus temperature for Crisitobalite ranges between 1200^oC to 1600^oC and increases with an increase in silica.

2.4.7   The FeO-Fe_2O_3-SiO_2-CaO System

This system is looked at for comparison puroses since it doesn't contain any chromium. Kongoli and Yazawa defined the liquidus surface of a FeO-Fe_2O_3-SiO_2-CaO system using thermodynamic modeling [24]. As part of their research they tested their findings against previous research and in most cases
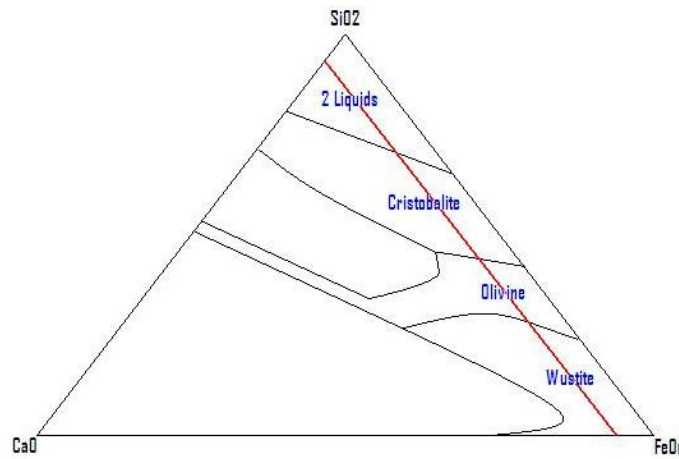
Figure 2.14: The SiO_2-FeO_x-CaO phase diagram. The original phase diagram was published in the Slag Atlas [23].

the model proved to be accurate. Using their model they investigated the effect of additives on the FeO-Fe_2O_3-SiO_2-CaO system under a log oxygen partial pressure of -8 atm. From the data produced by the model they constructed a polythermal projection diagrams (technology from Flogan Engineering). The specific additives investigated and the effect of each is discussed below.
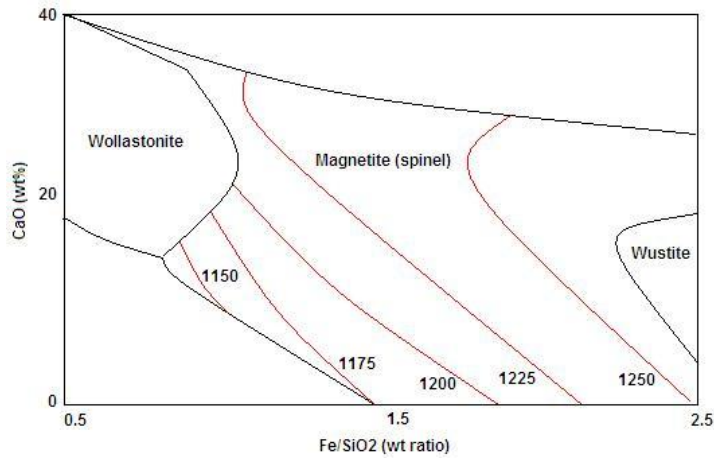
The effect of lime additions

The polythermal diagram can be seen in figure 2.15. In the figure there are four major zones, the silica saturated zone, the Wollastonite zone, the Wustite zone and the Magnetite (spinel) zone.

It can be seen from the diagram that in the Magnetite zone an increase in lime does not decrease the liquidus temperature. Kongoli and Yazawa [24] reported that at a constant Fe/SiO_2 ratio a weight percentage increase of lime resulted in an increase in the liquidus temperature (1%wt lime resulted in a 4^oC - 5^oC increase). This fact implies that an addition of lime can increase the probability of spinel formations (magnetite precipitation) [24].

Another important observation is that in the silica rich zone an addition of lime leads to lower liquidus temperatures. At this point an increase of 1%wt of lime resulted in a lowering of 40^oC-50^oC in the liquidus temperature [24].

The effect of Al_2O_3 additions

Kongoli and Yazawa [24] added to their research the effect of Al_2O_3 on the liquidus temperature of the FeO-Fe_2O_3-SiO_2-CaO system by using their thermodynamic model. The data produced by the model was fitted on a polythermal projection (shown in figure 2.16). In this figure the important crystalline area is the spinel area.

Figure 2.15: The effect of CaO addition on the CaO-FeO-Fe$_2$O$_3$-SiO$_2$ slag system. The diagram was adopted from the work done by Yazawa and Kongoli [24]
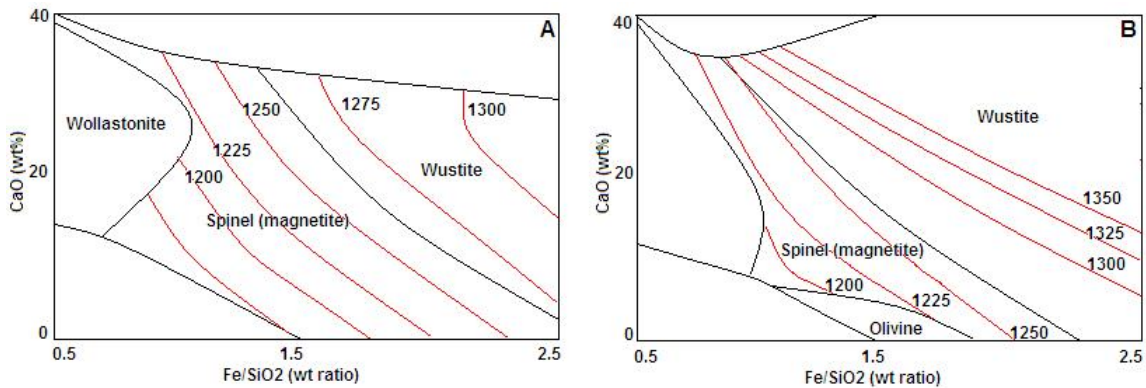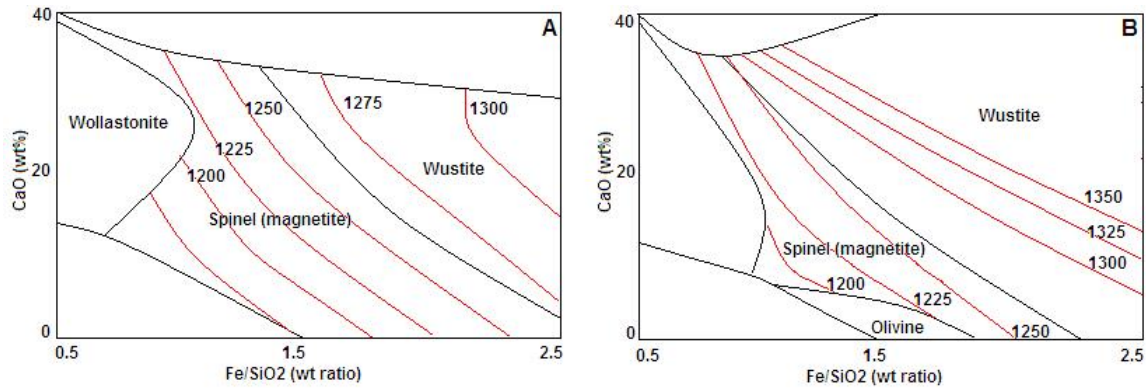

Figure 2.16: The effect of Al$_2$O$_3$ additions on the FeO-Fe$_2$O$_3$-SiO$_2$-CaO-Al$_2$O$_3$ slag system. The diagram was adjusted from the work done by Yazawa and Kongoli [24]

In figure 2.16 diagram A represents a 3%wt Al$_2$O$_3$ addition and diagram B represents a 7%wt Al$_2$O$_3$ addition.

From figure 2.16 Kongoli and Yazawa reported that an increase in the weight percentage of Al$_2$O$_3$ at a constant Fe/SiO$_2$ ratio will increase the liquidus temperature (1wt% Al$_2$O$_3$ equals 6°C - 8°C). Kongoli and Yazawa also stated that Al$_2$O$_3$ at a constant Fe/SiO$_2$ ratio will only lower the liquidus temperature near the silica rich phase. The last observation from figure 2.16 is the formation of an olivine phase at the lower lime additions and may also and may also be of interest in the current study [24].

Figure 2.17: The effect of MgO additions on the FeO-Fe$_2$O$_3$-SiO$_2$-CaO-MgO slag system. The diagram was adjusted from the work done by Yazawa and Kongoli [24]

The effect of MgO additions

The polythermal diagram for the addition of MgO is given below in figure 2.17. The important crystalline structures in figure 2.17 are the olivine and spinel-magnetite. Figure 2.17 shows two diagrams. Diagram A corresponds to a MgO addition of 3%wt and diagram B corresponds to a MgO addition of 7%wt.

As with the previous additives an increase in the weight percentage of MgO also lead to an increase in the liquidus temperature (1%wt of MgO gives a temperature rise of 7°C - 9°C). Compared with the previous polythermal diagrams considered in Kongoli and Yazawa research [24] the addition of MgO lead to the formation of olivine. They also stated that a 3%wt percentage of MgO stabilizes the formation of the olivine crystalline structure.

2.4.8   The FeO-Fe$_2$O$_3$-MgO-SiO$_2$ System

In the FeO-Fe$_2$O$_3$-MgO-SiO$_2$ sytem there exists a molten oxide phase, a monoxide (FeO-FeO$_{1.5}$-MgO) phase, iron-magnesium spinel, Olivine (incompassed by forsterite and fayalite) and Pyroxenes (refer to figure 2.18). The FeO-Fe$_2$O$_3$-MgO-SiO$_2$ system shows a liquid phase at a temperature of 1687°C and a silica content greater than 70wt%. By lowering the silica content at a constant MgO/Fe$_3$O$_4$ ratio, olivine and ortho-pyroxene starts to form. At this point the liquidus temperature ranges from 1200°C to 1800°C depending on the MgO and Fe$_3$O$_4$ content.

Keeping the MgO/Fe$_3$O$_4$ ratio constant and lowering the SiO$_2$ below 20%wt results in the formation of Magnesiowustite. The liquidus projections for this phase are estimated between 2000°C and 2800°C [25].
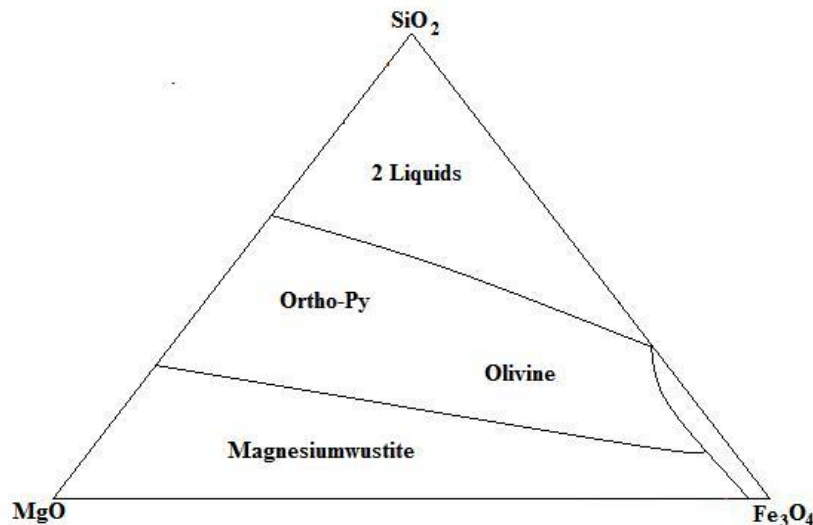
Figure 2.18: A simplified MgO-SiO$_2$-Fe$_3$O$_4$ phase diagram adopted from Jung, In-Hu et.al [25]

2.5 The prediction of thermodynamic properties for multicomponent systems

Research has been conducted in the development of model equations that would be able to predict the Gibbs free energies for different phases based on the composition and temperature of the system. This is called thermodynamic "optimization" [26]. The "optimization" entails the simultaneous evaluation of thermodynamic and phase equilibrium data in order to calculate all the parameters needed to obtain one set of model equations that would predict the Gibbs free energies for a system [27].

A modified quasi-chemical equation was developed for the excess molar Gibbs energies since the use of polynomial expansions are inadequate for liquid SiO$_2$, which forms a highly ordered system [27]. Since the purpose of this project is not the development of the quasi chemical model, only a brief outline will be discussed for a binary system. Consider a molten oxide solution with components AO and BO. If the formation of two second-nearest-neighbor bonds (A-B) are assumed the reaction can be expressed as [26]:

$$(A - A) + (B - B) = 2(A - B) \tag{2.12}$$

Defining Y$_{AA}$,Y$_{AB}$ and Y$_{BB}$ as fractions of the different bonds it is possible to derive two mass balances (see equations 2.13 and 2.14) and an equilibrium constant (see equation 2.15).

$$2(Y_{AO}) = 2(Y_{AA}) + Y_{AB} \tag{2.13}$$

$$2(Y_{BO}) = 2(Y_{BB}) + Y_{AB} \tag{2.14}$$

$$\frac{Y_{AB}^2}{Y_{AA}Y_{BB}} = 4exp\left(\frac{-2(\omega - \eta T)}{zRT}\right) \tag{2.15}$$

From these equations thermodynamic properties such as entropy can be defined, for example [26] [28],

$$\Delta H = (b_{AO}Y_{AO} + b_{BO}Y_{BO})\left(\frac{Y_{AB}}{2}\right)\omega \tag{2.16}$$

The same can be done for nonconfigurational entropy of mixing and configurational entropy of mixing [26]. From equation 2.15 and equation 2.16 the greek symbols, ω and η, were expanded as polynomials (see equation 2.17 and equation 2.18).

$$\omega = \omega_0 + \omega_1 Y_{BO} + \omega_2 Y_{BO}^2 + \omega_3 Y_{BO}^3 + ... \tag{2.17}$$

$$\eta = \eta_0 + \eta_1 Y_{BO} + \eta_2 Y_{BO}^2 + \eta_3 Y_{BO}^3 + ... \tag{2.18}$$

It is these coefficients, ω and η, that is determined from thermodynamic "optimization". In order to optimize a multicomponent system the first step is to optimize the binary system. Then by using that information ternary systems and in the end the multicomponent system as a whole, can be optimized.

FactSage^{TM} incorporates these equations when making thermodynamic predictions, this means that FactSage^{TM} predictions is based on optimized binary and ternary systems. To add confidence to FactSage^{TM} predictions the optimization and validation of the binary and ternary systems have to be investigated to evaluate the different ranges such as temperature and composition.

The CaO-FeO, CaO-MgO and FeO-MgO system was optimized by Ping Wu et.al [26]. The FeO-MgO system was validated for a range between 1400^oC to 2400^oC. The reported maximum probable inaccuracy was 100^oC. The MgO-CaO binary system a eutectic point was observed at 59mol% and a temperature of 2360^oC. The optimized phase diagram was accurately validated for a temperature range of 1500^oC to 2800^oC and the maximum probable error was reported to be 50^oC. Investigating the CaO-FeO phase diagram, a eutectic point was found at a temperature of 1125^oC and 73% FeO. The reported maximum probable error of 2mol% was reported over a temperature range of between 1050^oC to 1800^oC [26].

Erikson and Pelton [27] optimized the CaO-Al$_2$O$_3$ and Al$_2$O$_3$-SiO$_2$ systems. For both the CaO-Al$_2$O$_3$ and the Al$_2$O$_3$-SiO$_2$ system an inaccuracy of 25^oC or 2mol% within an temperature range of 1500^oC and 1780^oC were observed [27]. After the quasi model proved to be accurate on the binary and ternary

systems, it was extended to quaternary systems such as the MgO-Al$_2$O$_3$-CrO-Cr$_2$O$_3$ and the FeO-Fe$_2$O$_3$-MgO-SiO$_2$. Accuracies for the quaternary system models are not reported but these models are seen as the best representation of the thermodynamic properties of these system [29].

A ternary Fe-Ni-S matte system was optimized by Waldner P, et.al [30]. In his research the modified quasi chemical model was combined with the extended modified quasi chemical model and sub lattice models were added to take into account ternary solid solutions such as pyrrhotite and pyrite. Validation of the model was conducted over a sulphur partial pressure range of log(pS$_2$)= 0 to log(pS$_2$)= -8 and a temperature range of 600°C to 1400°C. They reported that the new combined model permits very good predications and concluded that the optimized data obtained could be used for optimizing a higher order multicomponent system [30].

To conclude, the quasi chemical model is very successful in the modeling of thermodynamic properties for both sulphur and oxide mixtures. The accuracies however were tested on each mixture separately and not in conjunction.

2.6 The physical properties of the iron-silica-lime system and spinel

In this section the change in physical properties such as the density, surface tension and viscosity of the FeO-Fe$_2$O$_3$-SiO$_2$-CaO as a function of lime additions is discussed. The second part of the section discusses the spinel structure and different types of spinel.

2.6.1 The physical properties of the iron-silica-lime system

Vandsz reported a density range for the FeO-Fe$_2$O$_3$-SiO$_2$ system (3.5g.m^{-3} and 4.25g.m^{-3}) at a temperature of 1000°C and a composition of 30%wt SiO$_2$, 20%wt Fe$_2$O$_3$ and a FeO weight percentage greater than 50%wt [31]. It was also reported that an increase in the SiO$_2$ content resulted in a decrease in the density while Fe$_2$O$_3$ had the opposite effect. For the same type of slag a surface tension between 350 mN.m^{-1} and 475 mN.m^{-1} were reported. Vandasz stated that the surface tension increased with the addition of both SiO$_2$ and Fe$_2$O$_3$ [31] . The viscosity for this slag was found to range between 50mPa.s and 500mPa.s. It was found that the viscosity of the slag increased with an increase in Si^{4+} and Fe^{3+} complexation cations [31].
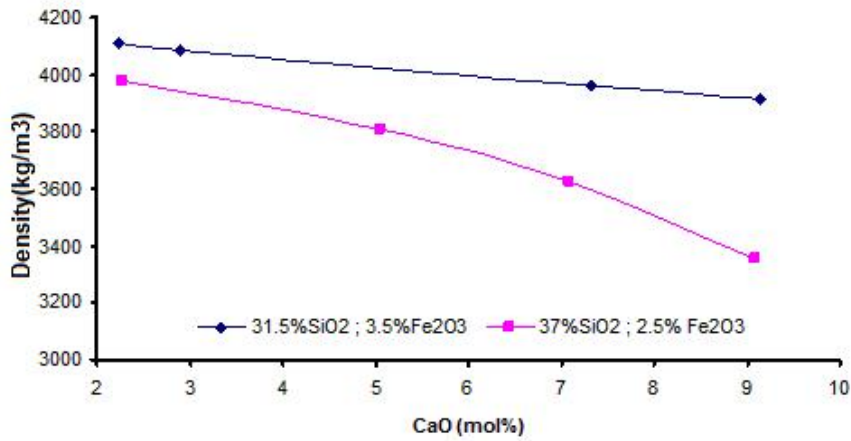
Figure 2.19: The effect of CaO additons on the density of the iron-lime-silica system [31]

The effect of lime on the density

In Figure 2.19 it can be seen that an increase in lime content causes a decrease in the density. The effect is less severe for the slag containing more SiO_2 and less Fe_2O_3.

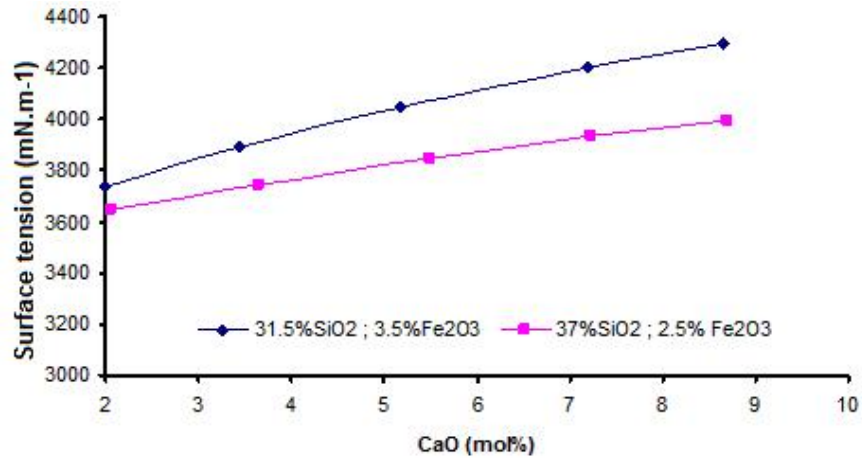## The effect of lime on the surface tension

The surface tension is important in this study since the surface tension could influence the distribution of compounds across the slag and matte interface. Figure 2.20 shows the effect of lime addition on the surface tension of a FeO-Fe_2O_3-SiO_2 melt. From figure 2.20 it is evident that an addition in lime leads to an increase in surface tension for both types of slag compositions. The figure shows that a CaO increase of 8%wt leads to a surface tension increase of 18%wt.

The effect of lime and temperature on viscosity

In Figure 2.21 the melt containing less lime shows a higher viscosity than the melt containing more lime from a temperature of 1270^oC and higher. The figure also indicates that as the temperature of the melt increases the viscosity decreases.

2.6.2   The physical properties of spinel

This section will discuss the structure of the spinel compound and the reason why spinel is unwanted during furnace operation.

Figure 2.20: The effect of CaO additons on the surface tension of the iron-lime-silica system [31]
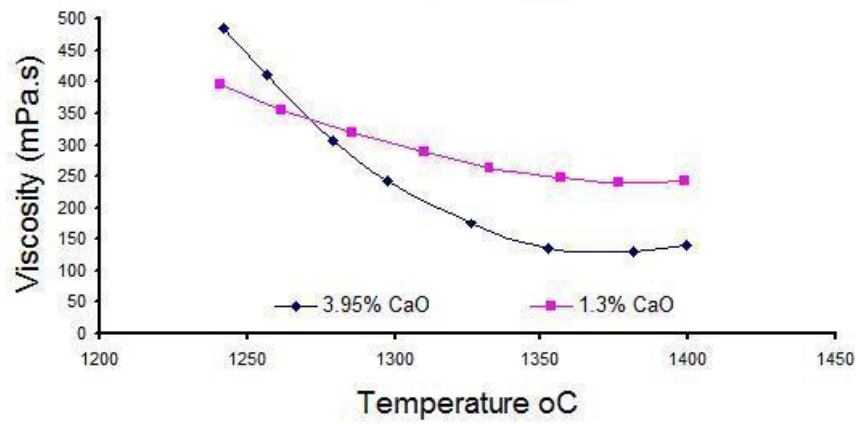
Figure 2.21: The effects of lime additions and temperature on the viscosity of the melt [31]

In 1915 it was discovered that chromium ores shows the same crystallographic structures as the spinel $MgAl_2O_4$. Most spinels can be represented by the formula, AB_2O_4. In the formula A represents divalent cations (Mg^{2+}, Fe^{2+}) while B represents the trivalent cations (Cr^{3+}, Al^{3+}) [32]. Other compounds have also been reported:

1. $A^{2+}B2^{3+}O_4$ Spinels occurring in this form are called 2-3 spinels

2. $A_2^{2+}B^{4+}O_4$ Spinels occurring in this forms are called 4-2 spinels

3. $A_2^{+}B^{6+}O_4$ Spinels occurring in this forms are called 6-1 spinels

The first cation coordination study for spinel was completed in 1930, this was also the first time that the complexity of the spinel structure became apparent. There exists two types of spinels, normal spinels and inverse spinels, due to the different cation arrangements [32].

In a normal spinel the octahedral sites are occupied with only one type of cation, in an inverse spinel half the octahedral sites are filled with the "A" type cation while the other half is filled with the "B" type cation. Chrome spinels are usually found to be of the normal type due to the large molecular weight of Cr.

Spinel structures have the following charateristics:

1. Spinel materials are seen as a refractory oxide which implicates that it is a stable compound and has a high melting temperature [32].

2. Specific heat capacities for chromium spinels can range from 40.5cal/mole/ ^oC up to 52.9 Cal/mole/^oC depending on the end-member of the spinel [32].

3. During the formation of spinels the radii of the cations can play a role in the type of end-member or compound that forms. For instance cations in the range of 0.44A to 1A may substitute to form chrome spinels. If the radii is less than 0.44A other compounds may form such as olivine [32].

4. During spinel crystallization impurities form inside the spinel structure. These impurities make it difficult to determine the actual resisitivity of the spinel to electrical flow, but research showed that as the chrome content increases the resistivity of the spinel also increases [32].

The effects of spinel on furnace operation

It was previously mentioned that spinel is seen as a refractory material. This means that it is a stable compound with a high melting temperature. Some of the effects of spinel formation on furnace operation include:

1. As the chromium content of the a slag increases the density of the slag increases as well [3]. This effect decreases the amount of separation between the matte and slag phase. If the separation between the matte and slag phase decreases the platinum group metal recovery to the matte phase decreases as well.

2. Chromium spinel inside a furnace can raise the liquidus temperature from 1300°C to 1600°C [7]. This fact is supported by Barnes [3] which states that a 5%wt increase in chromium oxide will raise the liquidus temperature of a MgO-Cr2O3-SiO2 slag to 1800°C. A higher liquidus temperature results in higher power consumption. The power requirments for melting just UG2 ore can increase from 896kWh/t at 1350°C to 1088kWh/t at 1450°C [1].

3. Buildup. The spinel in the intermediate zone (between the matte and the slag phase) tends to freeze when it touches the sidewall of the furnace and material starts to accumulate on the side walls. The same problem occurs when matte is tapped. This leads to the "intermediate zone" touching the hearth, forming spinel build up at the lower part of the furnace. Spinel build up lowers the furnace volume which, in turn, lowers the effective smelting volume [7]. Barnes [3] states that build up has an affect on the matte tapping cycle and that continuous build up can eventually terminate furnace operation.

Chapter 3

Project scope and procedure

This chapter discusses the problem statement and from the problem statement and the literature review hypothesis were made and the objectives for this project were determined.

3.1 Problem statement

In the theoretical background it is evident that the platinum production companies are facing a major problem concerning chrome based platinum ore. Chrome-bearing ore leads to problems such as high liquidus temperatures, spinel formation and problems in the converting stage. Therefore, there are fiscal implications for companies which processes chrome bearing platinum ores without much understanding the behaviour of chrome in their furnaces. Listed below are a several stragegies that companies could follow to process high chrome bearing ore.

1. Companies can either continue melting chrome bearing ore as they would have processed conventional ores. However, this will lead to spinel formation which in turn lowers furnace volume and could result in terminating furnace operation.

2. Companies could make alterations to a furnace in order to be able to work at higher temperatures. With higher temperatures more spinel enter the matte pahse due to dissolution.

3. Another probable solution is presented by Barnes [3] it entails the selective solidification of oxides. Some issues concerning another tap hole between matte and slag tap holes can make this solution a logistic nightmare.

4. Companies could also adjust the current production process by altering electrode depth, slag chemistry or tapping frequency.

This research project forms part of the solution to alter electrode depth, slag chemistry or tapping frequency by investigating the effect of altering the slag chemistry on chrome deportment. Lime was added to the platinum production process to lower the liquidus temperature of the melt and to decrease the viscosity [3]. However, common practice today is to operate the furnaces at higher temperatures which makes the higher lime additions unnecessary.

3.2   Hypothesis

From the literature review and problem statement the following hypothesis were drawn.

1. *Chrome deportment between a matte and a slag phase can be successfully investigated using a synthetic oxide/sulphide system.*

2. *Slag additives such as lime and silica will influence chrome deportment in all the phases that will be present at equilibrium.*

3. *Basicity, or the interaction between oxides, will influence chrome deportment between the phases present at equilibrium.*

3.3   Objectives

The following objectives were identified for this research project.

1. To successfully simulate a matte/slag phase inside a tube furnace using an alumina crucible and a controlled atmosphere.

2. To determine the reaction time that is required to come as close to equilibrium as possible.

3. To reduce the amount of chromium deporting from the slag phase to the matte phase.

4. To investigate if basicity has an effect on chrome deportment.

5. To try and validate the results obtained from FactSage^{TM} (thermodynamic predictions).

Chapter 4

Experimental Procedure

In this study chrome deportment between a slag / matte system similar to the compositional ranges encountered in the platinum industry was investigated using a vertical tube furnace. To simulate a matte phase a controlled atmosphere needs to be maintained and this was achieved using a combination of four different gasses (CO, CO_2, SO_2 and Ar). After the sample spent the required reaction time in the furnace it was drop quenched and prepared for analysis.

This section will describe all the equipment that was used for experimentation and methods in material preparation that were used in the project. The validation of the equipment will also be discussed.

4.1   Experimental equipment and methods

A gas rig was used to remove traces of moisture and carbon dioxide, using silica gel and lime respectively, from the gasses entering the vertical tube furnace. The gas train consisted out of a digital set point controller, digital mass flow controller and four sets of cleaning chambers. The mass flow controllers were activated an hour before an experimental run started to ensure that the mass flow controllers were at steady state (Prescribed in mass flow controller's manual) supplying a homogenous mixture that fills the entire gas train. The gas mixture from the gas train was then passed into a copper chip furnace. This is a furnace that contains copper chips (turnings) heated to 500°. Any trace amounts of oxygen in the gas stream took part in an oxidation reaction with the copper and was subsequently removed from the gas stream. The gas mixture was then passed through a mixing chamber to ensure homogeneity of the gas before it was injected into the vertical tube furnace.

The vertical tube furnace (figure 4.2) is the main equipment that was used for phase equilibria studies. A vertical tube furnace consists of a vertical ceramic tube surrounded by 6 silicon carbide elements. What makes the tube
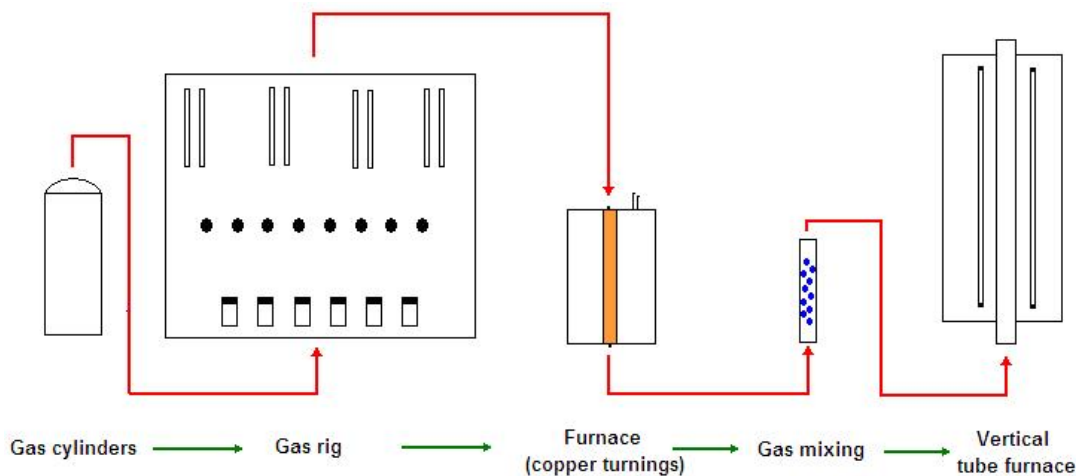
Figure 4.1: The experimental setup used for chrome deportment studies

furnace so exceptional is the fact that the tube can be completely sealed of from the surrounding atmosphere which is necessary to achieve a certain gas atmosphere. On top and bottom of the ceramic tube is a water cooled flange that cools the O ring needed to seal the furnace. Connected to the flange is the radiation shield. The gas line entering the tube furnace is connected to the bottom flange. Before the sample was loaded the temperature of the furnace was lowered to 1400^oC, this was necessary to prevent the gas mixture from attacking the guide wire [33].

With a homogenous gas entering the tube furnace it was then possible to load the sample. A guide wire, made out of platinum, was lowered through the top radiation shield right through and out at the bottom of the furnace, a sample wire (the wire that holds the sample in the hotspot of the furnace see subsection 4.1.1) is connected to the guide wire. A "cage" also made out of platinum wire was used to secure the crucible onto the sample wire. With the sample inside the crucible the guide wire was hoisted up until the crucible just entered the furnace. At this point the furnace was sealed off at the bottom radiation shield and thirty minutes were given for the gas mixture to fill the ceramic tube (calculations showed that ten minutes would have been sufficient).

After thirty minutes the sample was hoisted at a rate of approximately 15mm/min. This rate was chosen to ensure that the crucible doesn't form hairline crakes that could lead to possible burn-troughs, the slow hoisting rate also ensured that gas formation was slow enough to prevent the mixture inside the crucible from spilling over. When the sample was in the furnace hot spot the furnace was sealed off at the top radiation shield and the temperature of the furnace was raised at 2^oC/min to the desired temperature. Upon reaching that temperature the reaction time measurement was started.
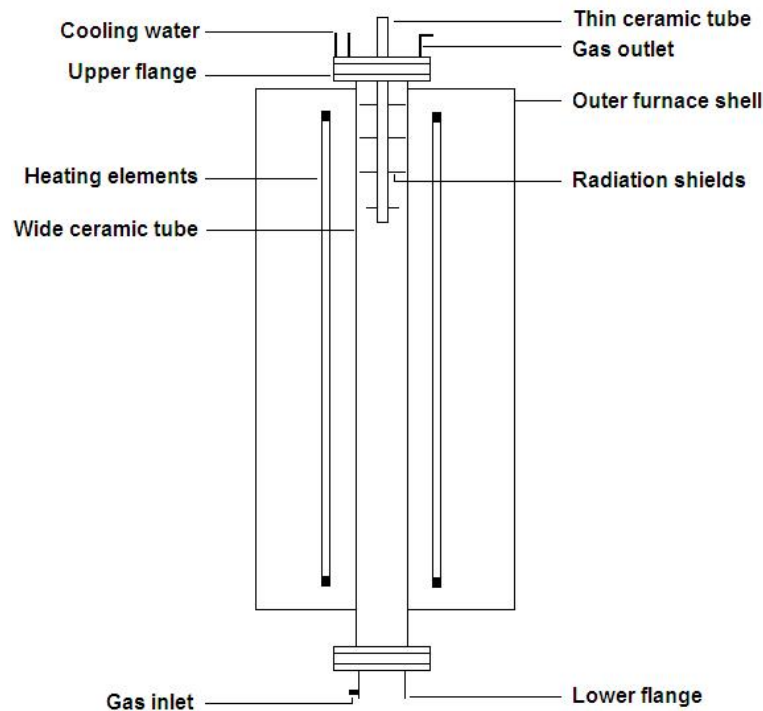
Figure 4.2: The detailed vertical tube furnace

### 4.1.1   Validation of temperature inside the tube furnace

The temperature inside the tube furnace was verified using an R type thermocouple. This thermocouple was calibrated using the method discussed by [34].

The method is based on a thermodynamic principle which states that the temperature of a substance or species remains the same as the speciec or substance undergoes a change in phase [35]. The thermocouple was calibrated using copper as a reference material. The copper was placed in an alumina crucible inside a muffle furnace. The copper was heated to 1140°C which is 50°C above its melting temperature. At that point the furnace was switched off and the uncalibrated thermocouple was used to take temperature readings every ten seconds up until the temperature reading was a hundred degrees less than the melting temperature of copper.

A cooling curve was created by plotting the temperature versus time data. Figure 4.3 illustrates the copper cooling curve. In the cooling curve the copper was heated to 1140°C at time zero. At time zero the furnace was switched off and the material started to cool down. As time progresses the cooling curve forms a plateau, at this point the copper was starting to solidify (thermodynamic principle: during phase change the temperature will remain constant).
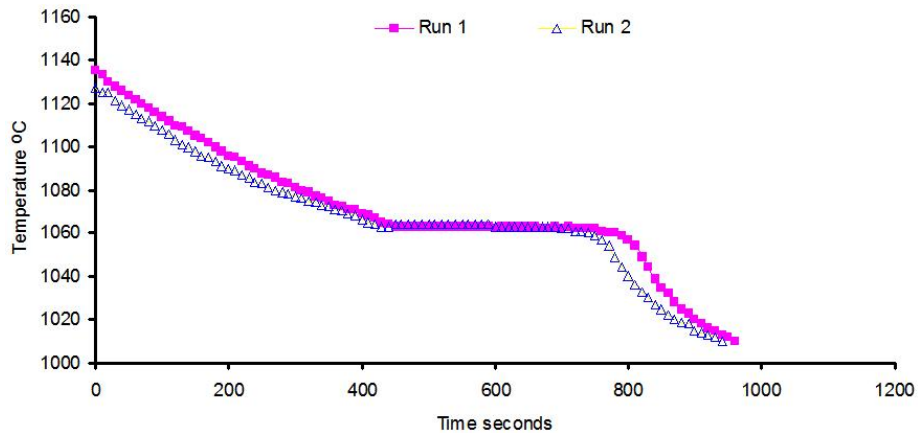
Figure 4.3: The copper cooling curve
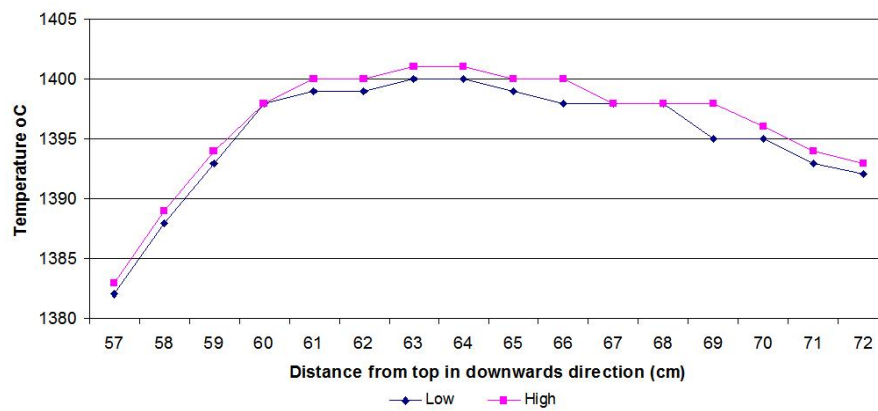
Figure 4.4: Temperature profile inside the Vertical tube furnace

From figure 4.3 the uncalibrated thermocouple indicated that the copper solidified at 1060°C which is twenty degrees lower than the actual melting temperature of copper. This means that there was a twenty degree difference between the temperature that the uncalibrated thermocouple detected and the actual temperature. The thermocouple was adjusted accordingly.

It is important to note that a tube furnace has a temperature profile across the length of the tube. This profile was determined prior to the experimenting. The tube furnace also had a heating cycle, meaning that the temperature at one point had a low and a high value. From figure 4.4 the hot spot in the furnace was estimated to be 62cm into the furnace (measured from the top radiation shield). All the crucibles were suspended in the hot spot to ensure that they were at the correct temperature.
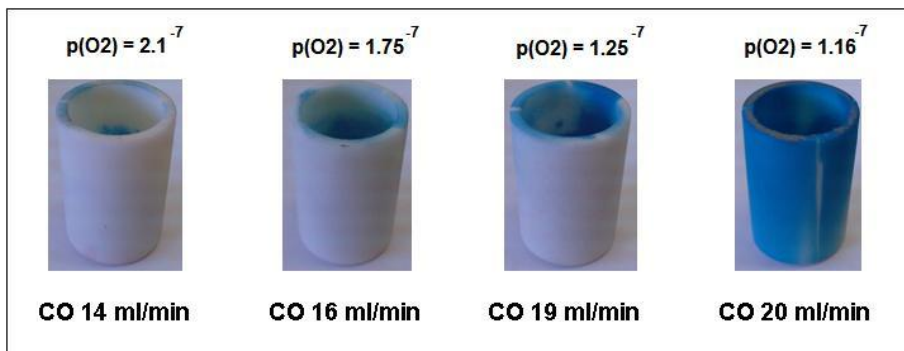
Figure 4.5: The reduction of nickel oxide

4.1.2 The oxygen and sulphur partial pressures inside the tube furnace

The correct partial pressure of sulphur and oxygen inside the tube furnace was maintained using a mixture of four gasses namly. argon, carbon dioxide, carbon monoxide and sulphur dioxide. Equations 4.1 and 4.2 shows the chemical reactions that are involved.

$$2CO_2 \Leftrightarrow 2CO+O_2 \tag{4.1}$$

$$SO_2+CO \Leftrightarrow S_2+CO_2 \tag{4.2}$$

The amount of each gas needed to create the desired atmosphere was calculated using FactSage^{TM}. Knowing what the correct theoretical gas flow rates should be, the mass flow controllers were adjusted accordingly using a bubble flow meter. With the bubble flow meter the gas flow rate was measured by determining the time it takes for a film of soap to travel a known length inside a glass tube. The known length is associated with a certain volume and was used to calculate the flow rate.

With the gas flow rates validated the oxygen partial pressures inside the furnace could be validated. The oxygen partial pressure were validated with the reverse equilibrium approach [36]. Nickeloxide (dark coal color) was reduced to Ni (gold in color) by maintaining the correct oxygen partial pressure (refer to equation 4.3).

$$NiO+CO=Ni+O_2 \tag{4.3}$$

A partial pressure of $p(O_2) = 1.75^{-7}$ is needed to reduce nickel oxide. However, from figure 4.5 it is evident that the nickel oxide was only reduced at a partial pressure of $p(O_2) = 1.16^{-7}$. These results were deemed acceptable.

4.2 Selecting a suitable crucible

Selecting the suitable crucible is an important step in phase equilibria studies. Hume-Rothery discusses the different crucibles that are available. The choice in crucible was based on the following guidelines.
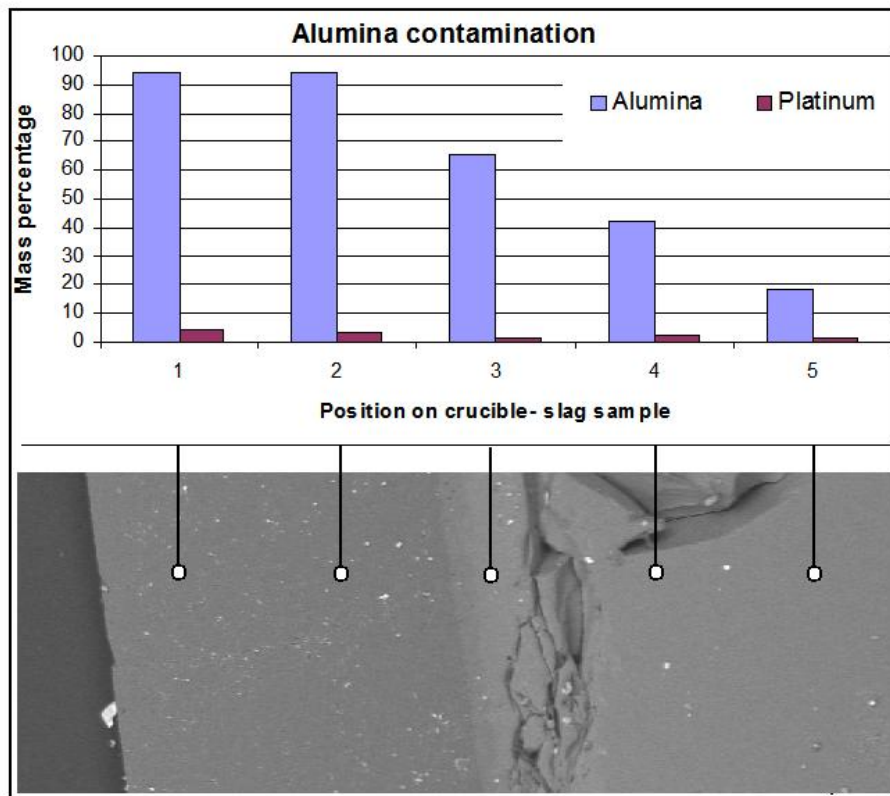
1. Temperature

2. Phases present

3. Effect on slag sample

4. Costs

5. Availability

The temperature of the system plays a role on the structural integrity of the crucible. For temperatures above 1500^oC the selection of crucibles included alumina, magnesia and platinum. For the system investigated in this study the combination of a slag / matte system eliminated the possibility of using a platinum crucible since the platinum is extremely soluble in a sulphide melt. This left the oxide crucibles as options, but all of these crucibles are to some extent soluble in the slag phase. Figure 4.6 shows the results of a solubility test conducted on an alumina crucible at 1550^oC in a typical unsaturated PGM slag after twelve hours. In the figure position 1 and 2 refers to the sidewall of the crucible and point 4 and 5 to the slag phase. The figure also indicates the that the sidewall containes platinum which could only come from the platinum wire used to suspend the crucible.

The results indicate that the alumina crucible is soluble in a unsaturated silica slag. Due to the solubility of the alumina crucible magnesia crucibles, were considered. However Mintek stated that the effect of additional alumina will not affect the results obtained in this project as much as magnesia crucibles and stated that they use sintered alumina crucibles for their studies. Mintek also advised on the necessity of saturating the slag system with 15%wt alumina [37].

4.3 System investigated and experimental design

The system investigated consisted of a matte and a slag phase that covers a wide range of different slag systems including the typical slag compositions found in the platinum industry. Variations were made on the lime, silica and chrome content of the feed to help clarify the effect of different slag additives on chrome deportment.

Figure 4.6: The inteface between an alumina crucible and the slag phase

Silica	Lime	Chrome	Temperature
30.0%	2%	1%	1550°
38.3%	5.3%	2.3%	x
46.6%	8.6%	3.5%	x
x	12%	x	x

Table 4.1: The different levels of slag additives that were investigated in this project

However, due to the fact that the slag needed to be saturated with alumina (refer to section 4.2) some of the effects of lime, silica and chrome additions could be suppressed. This meant that the mixtures being investigated were not representative of the slags systems found in the industry. The experimental runs in the tube furnace could therefore only be used to validate the trends predicted by FactSage^{TM}. The different levels of additives investigated are listed in table 4.1.

4.4 Materials and Preparation of Sample Mixtures

This section covers the methods that were followed to promote accurate experimental results. These methods are listed in [].

All the materials used had a purity of 99.95% and higher. Drying was the first step in the homogenizing of the different oxides (not including wustite) that were to be used. Listed below are the temperature and time requirements that were followed for each different oxide to ensure that it contained no moisture or crystal water.

1. SiO_2. Silicon dioxide was heated and kept at 1500^oC for two hours to remove any liquid inclusions.

2. Al_2O_3. Alumina was heated to 110^oC and kept at this temperature for three hours to remove any moisture.

3. $CaCO_3$. Calcium carbonate was used as a source of lime and was dried at 500^oC for five hours.

4. MgO. Magnesium oxide was heated 1050^oC to remove any moisture and to ensure that all the carbonates were decomposed.

After the oxides were dried the correct amounts were weighed, using a scale that is accurate to the third decimal, and were then thoroughly mixed in a mortar and pestle until a uniform color was obtained. Oxide mixtures were prepared with a total size of eleven grams to lower any weighing errors . The oxide mixture was then placed in a graphite crucible and heated to 1550^oC and kept at this temperature for four hours to obtain a uniform oxide melt. After the heating cycle the oxide mixture were pulverized using a ring mill. Contamination was prevented by "washing" the ring mill with silicon dioxide. The pulverized oxide mixtures were then sent for XRF to confirm whether the composition was correct.

For the sulphides a homogenous mixture(NiS, FeS and CuS) that were used for all the different oxide mixtures were prepared in ten gram batches (to emsure accuracy) by accurately weighing the material and by thoroughly mixing the material in a mortar and pestle. For the final sample the oxide mixture, wustite, sulphides and additional alumina were all thoroughly mixed together. During the weighing of mixtures (oxides, sulphides and final sample mixture) a representative sample was ensured by not scooping a single heap of material from the mixture but rather taking three smaller scoops. The mixture was also thoroughly mixed after each scoop that was taken.

4.5   Equipment and software used

4.5.1   Analysis

Analysis was done at Mintek in South africa, Mintek were chosen since they are very experienced in analysis of similar samples. Samples were analysed using a scanning electron microscope (SEM). Where averages was scanned an area of 190μm by 190μm) was typically used.

The mineralogy of the species were determined from the matching the SEM results to the stoichiometry of the species that were expected to be present.

4.5.2   FactSage

FactSage were used for the thermodynamic predictions. Only elemental component of the species were entered into Factsage and not the mineralogy of the species. A pressure of atmosphere were used. Duplicate results were suppresed and the following solution models were used:

1. Matte 2 were chrome is included in the matte phase

2. Slag A which contains all the oxide species

3. Olivine

4. Spinel

5. Pyroxene

Results were exported to excel were it was further processed.

4.6   Equilibration studies

Equilibration studies were conducted to determine the time needed for samples to reach equilibrium inside the furnace. Equilibration time needed is dependent on the properties, such as activity and viscosity, of a specific phase and the temperature of the system. For example, a matte phase would achieve equilibrium relatively quickly due to its low viscosity. In research conducted on a nickel sulphide in contact with a gas phase, equilibrium was achieved after only six hours [14]. Kaiser [38] investigated the equilibration time needed for a copper, iron and nickel matte and his results showed that equilibrium was achieved after 12 hours [38].

The slag phase on the other hand takes more time to reach equilibrium and is usually premelted to ensure homogeneity and to speed up the equilibrium process. In Bartie's [3] research on an alumina-chromium-iron-lime-magnesia-silica system he stated that equilibrium is only reached after 20 hours

Table 4.2: The Composition of sample no.27 prior to equilibration

Cr_2O_3	CaO	SiO_2	Al_2O_3	MgO	Sulphides + FeO
3.5	2.0	46.6	3.1	15.9	Balance

at 1400^oC. However, the composition of the slag after 4.7 hours only changed significantly for certain species such as chromium content (in glass phase) and silica. Another investigation on magnesia in an calcium ferrite slag showed that equilibrium was reached after 12 hours at a temperature of 1300^oC.

The spinel phases which are very viscous with high melting temperatures, where investigated. Jamieson [39], he found the distribution of Mg and Fe^{2+} between olivine and spinel reached equilibrium after 24 hours at 1300^oC [39].

From the above introduction it is clear that the time needed to achieve equilibrium is dependent on the phases present as well as the temperature of the system. In the introduction above there is no reference to an equilibration time needed for a system containing both the matte as well as the slag phase as is the case with the system investigated in this report. The reason therefore is that there is no crucible that could contain both the slag phase and the matte phase without interfering with either one of the phases. Any continual interference from the crucible would mean that equilibrium can not be reached. This is the case with the current system since the slag phase is continually dissolving the alumina crucible. Since equilibrium can not be reached it is necessary to estimate, not the equilibrium time needed, but rather a reaction time required, which entails the assumption that the system as a whole is not at equilibrium but rather the interface between the matte and slag phase [14]. The reaction time should be sufficient for important trends to from but should not be too long for the increasing amount of alumina to form a non representative sample.

For the system investigated in this study slag mixture no 27 (refer to table 4.2)was chosen to perform the equilibration experiments on. Slag mixture no 27 contained a low amount of lime which meant it had a relativly high viscosity which meant an increased reaction time (when compared with the other slag mixtures).

Reaction time periods of 4, 7, 11 and 16 hours were used for the equilibration studies.

In figure 4.7 the first and most important observation is the continual increase of the alumina oxide content of the slag. The continual increase can be attributed to the alumina crucible, used for experimentation, that is dissolving into the slag phase and it will continue until equilibrium is reached between the slag sample and the crucible itself. With $FactSage^{TM}$ this state of equilibrium is estimated to be around an alumina content of 60%wt in the slag phase and from figure 4.7 this state is reached after sixteen hours. Samples with this high amount of alumina ,however, is not satisfactory since the high
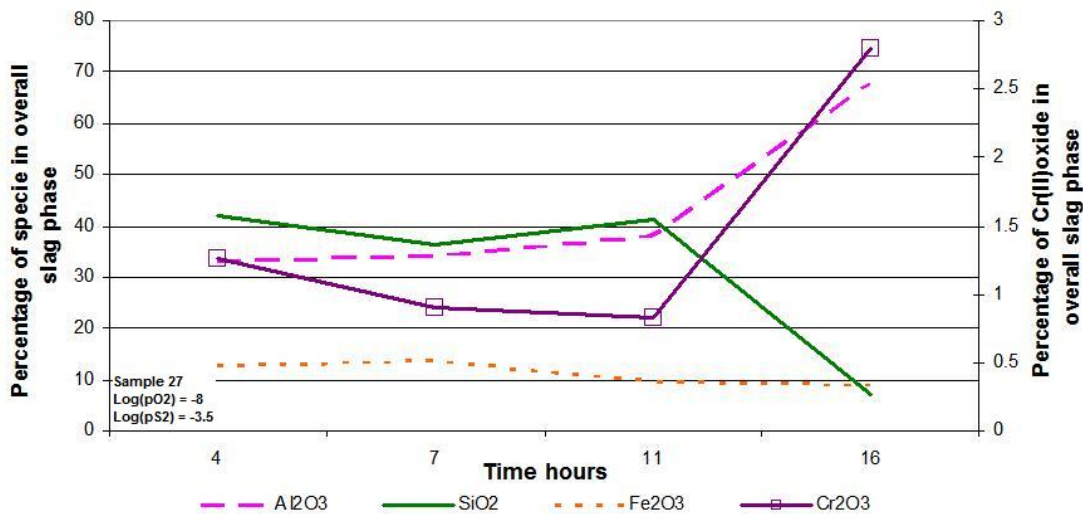
Figure 4.7: Changes in the slag composition as time progresses

amounts of alumina would eliminate some ,if not all, of the effects of the other manipulated variables such as lime addition. The reaction time needed for the species in the sample to reach equilibrium between themselves, and not the alumina crucible, was then investigated based on different observations.

In figure 4.7 the percentage of alumina in the slag phase stayed fairly constant between four and seven hours, whereafter the alumina started to increase. This is the most likely explanation for the trend reversal observed in the other species. From figure 4.7 another observation is that after eleven hours the slag's alumina content increased dramatically to an unacceptable level. This time was chosen as the maximum reaction time limit.

In the matte phase the different species stayed fairly constant between four and seven hours, whereafter the matte phase underwent significant changes and reached what seems to be equilibrium after eleven hours (refer to figure 4.8). Comparing figure 4.7 and figure 4.8 the reaction time should not exceed eleven hours but it is also evident that seven hours is not enough for the matte phase to achieve equilibrium. To confirm these findings a two point analysis was conducted on the sample to investigate the diffusion gradients within a phase for the different pahses (refer to figure 4.9 and figure 4.10).

In the slag, iron shows the smallest concentration gradients between four and seven hours. At eleven hours there is a 9%wt difference in the iron composition which decreased to 6%wt at sixteen hours. The iron concentration differences indicated that after eleven hours the composition of the different phases started to change. This could have been the result of the increase in alumina.

Also, chrome concentration gradients in the slag varied as time progressed (refer to figure 4.10). This was most likely due to chrome being a minor element
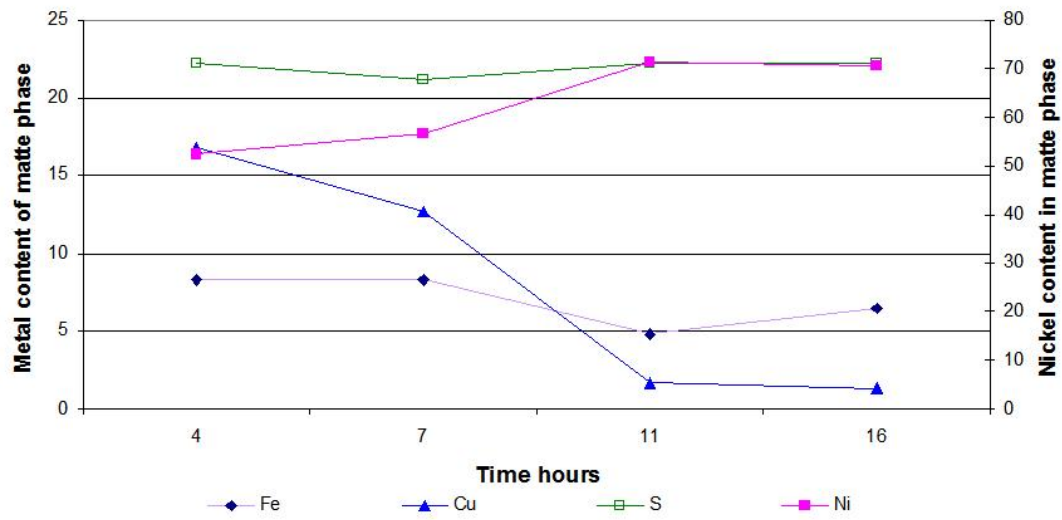
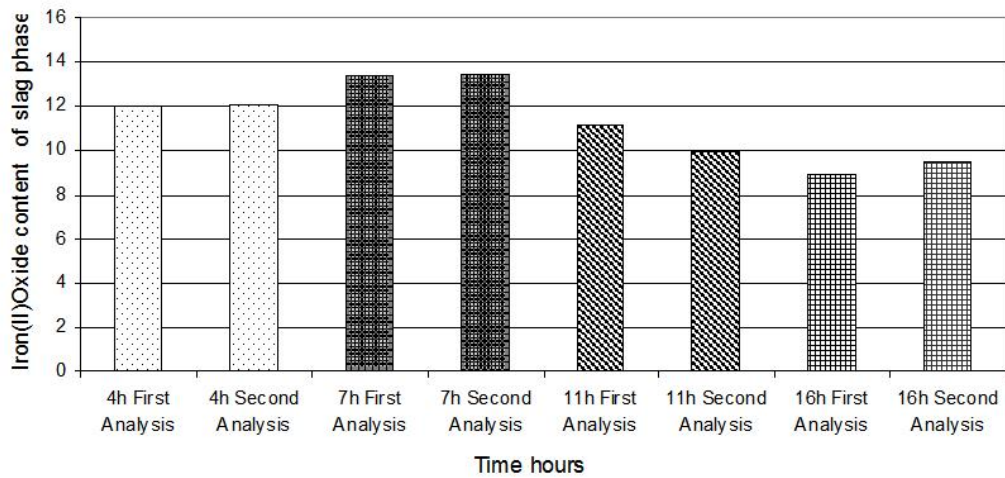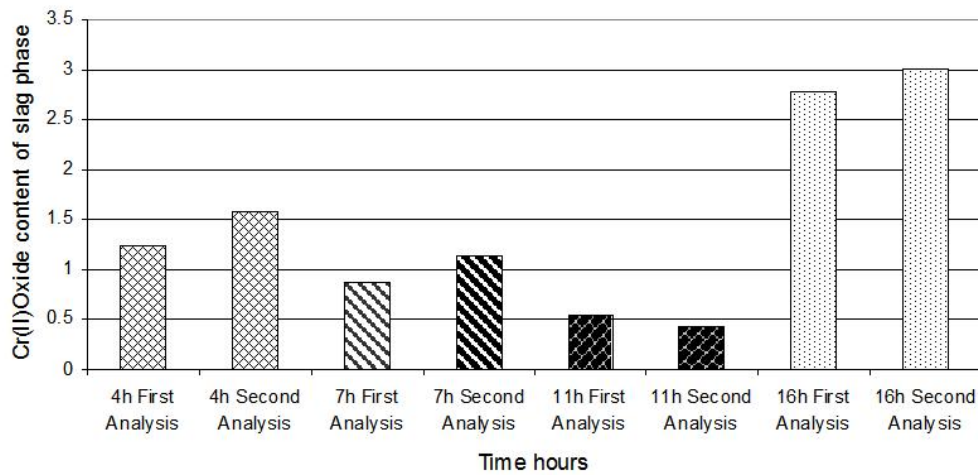**Figure 4.8:** Changes in the matte composition as time progresses

Figure 4.9: Two point analysis of IronOxide as time progresses

Figure 4.10: Two point analysis of ChromeOxide as time progresses

that could have distributed itself between the slag and matte phase. As the experiment started the matte phase contained zero chrome, creating a chrome diffusion gradient. The chrome then started to diffuse ,in small quantities, to the matte phase which lead to concentration differences in the slag phase. With time progressing alumina dissolved into the slag phase which formed a new concentration gradient allowing the chrome to diffuse back into the slag phase. This explained the concentration gradients over the entire time period.

Based on the findings above a reaction time of nine hours was chosen to give the matte sample enough time to react but to prevent the slag composition to change dramatically due to the alumina dissolution from the crucible.

Chapter 5

Discussion of Results

The objective of this study was to investigate the effect of different slag additives (chrome content of feed, lime additions and silica additions) on chrome deportment between the matte and slag phase but also between the spinel and glass phase. In this section the effect of these additives on chrome deported are plotted using experimental results. The results used in these plots are based on area averages (typically in the order of 190μm by 190μm)

From the samples (see appendix 6.3) three main phases could be seen a glass phase, spinel phase and a matte phase. The glass phase contained in the order of 30%wt to 42%wt silica depending on the sample. The matte phase contained in the order of 20%wt sulphur and compares well to figure 2.5 which is based on research by Kress [14].

Upon further investigation there were three "sub" phases present in the matte phase itself. These phases were a nickel rich phase, a copper rich phase and then a phase where the species are more balanced. The spinel phase were observed in all the samples except the samples containing a silica content of 39%wt and higher. The spinel phase contained mostly alumina-iron spinel but chrome-iron spinel was also observed.

5.1 The effect of the chrome content of the feed stream on chrome deportment

In the following section all experimentation was conducted at a temperature of 1550°C, an oxygen partial pressure of log(pO$_2$)= -8 and a sulphur partial pressure of log(pS$_2$)= -3.5. A slag composition of 33%wt silica and 12%wt lime in the feed stream was used (see appendix 6.3).

The investigation into the effect of the chrome content of the feed on chrome deportment revealed that an increase in chrome content resulted in an increase in the amount of chrome in the glass phase (see figure 5.1) as well as the spinel phase (see figure 5.2). From figure 5.1 an increase of 1.5%wt in the chrome
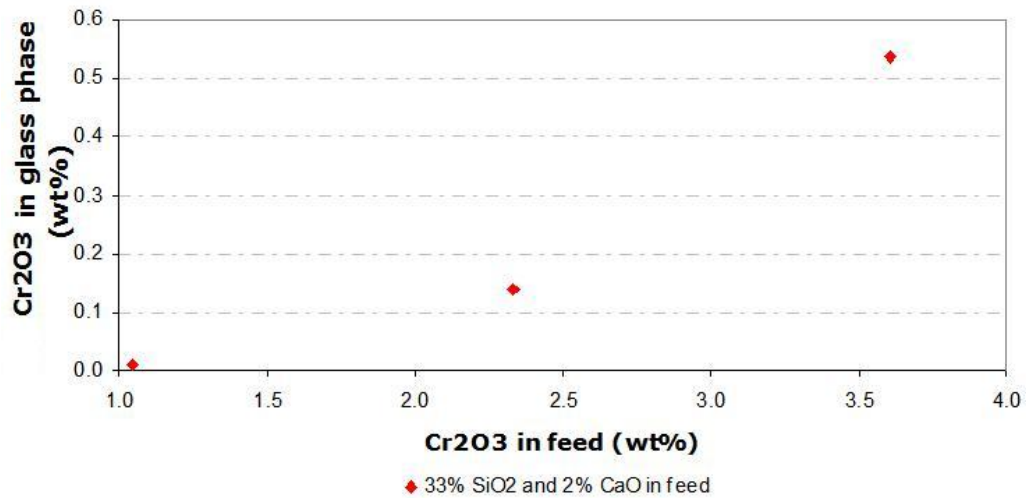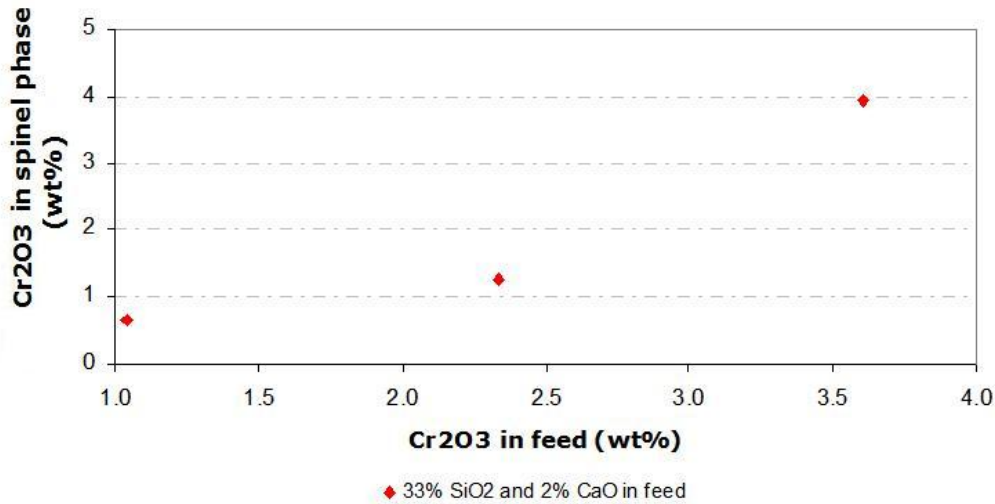
Figure 5.1: chromium oxide in the feed versus the Chrome content of the glass phase

content caused the chrome content of the glass phase to increase form 0.01%wt to 0.35%wt and shows a linear relationship. More important is that the figure shows the chrome content of the glass phase to still be increasing indicating the glass phase was not yet saturated with chrome. From figure 5.2 an increase of 1.5%wt in the chrome content of the feed causes the chrome content of the spinel phase to increase from 0.5%wt up to 2.6%wt and also follows a linear relationship.

For the matte phase, however, an increase chrome content of the starting material decreased the chrome content of the matte phase(see figure 6.10 in appendix 6.3).

Figure 5.2: chromium oxide in the feed versus the Chrome content of the spinel phase

5.2 The effect of the feed lime content on chrome deportment

The same experimental conditions were used to investigate the effect of lime in the feed stream on chrome deportment. Regarding the slag chemistry, a lime content of 1.7%wt and 10.1%wt were used at different silica levels (33%wt and 39%wt) while maintaining the other feed additives constant.

Figure 5.3 shows the effect of lime content of the starting materials on the weight percentage of chrome in the glass phase. The figure also shows two trendlines which represents the different silica levels. A large difference in chrome weight percentage in the glass can be seen between the slags containing higher silica levels and the slag containing lower silica levels. This may indicate that more chrome will disolve into the glass phase if the glass phase contains more silica. From the figure it is evident that an increase in lime will decrease the amount of chrome that dissolves into the glass phase. This effect of lime is also influenced by the amount of silica present. Figure 5.3 also shows that as the silica levels are decreased the amount of chrome dissolving into the glass phase decreases as well. For the 39%wt silica system an 6%wt increase in lime decreased the amount of chromium in the glass phase from 0.75%wt to 0.46%wt.

Figure 5.4 shows the effect of the lime content of the feed on the amount of chrome reporting to the spinel phase. In this figure the 33%wt silica system are shown since no spinel was found at silica levels of 39%wt. The guideline in this figure shows the opposite trend than figure 5.3. In this case, as the lime is
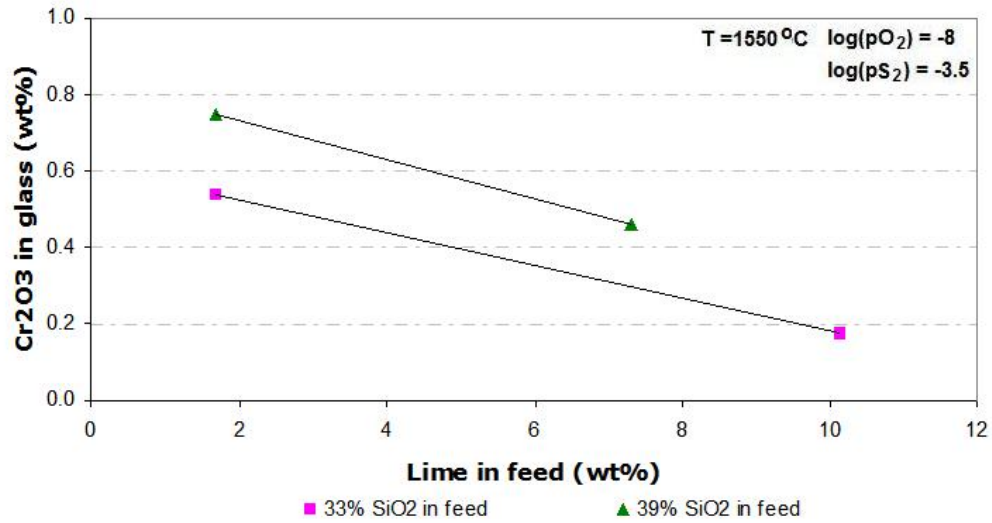
Figure 5.3: The relationship between the lime in feed stream and the chrome content of the glass phase
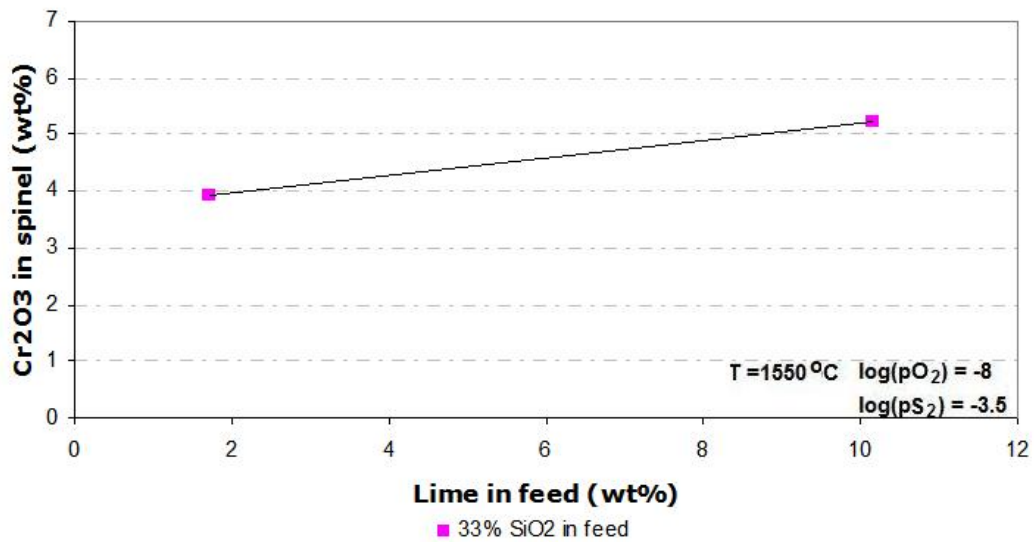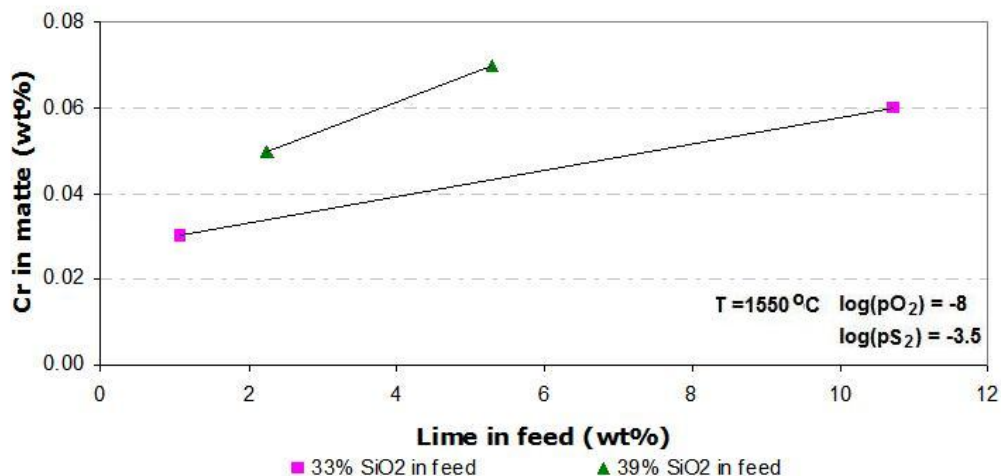

Figure 5.4: The relationship between the lime in feed stream and the chrome content of the spinel phase

Figure 5.5: The relationship between the lime in feed stream and the chrome content of the matte phase

increased the amount of chrome reporting to the spinel phase increases, for an 8%wt increase in lime the chrome content of the spinel phase increased from 3.9%wt to 5.2%wt.
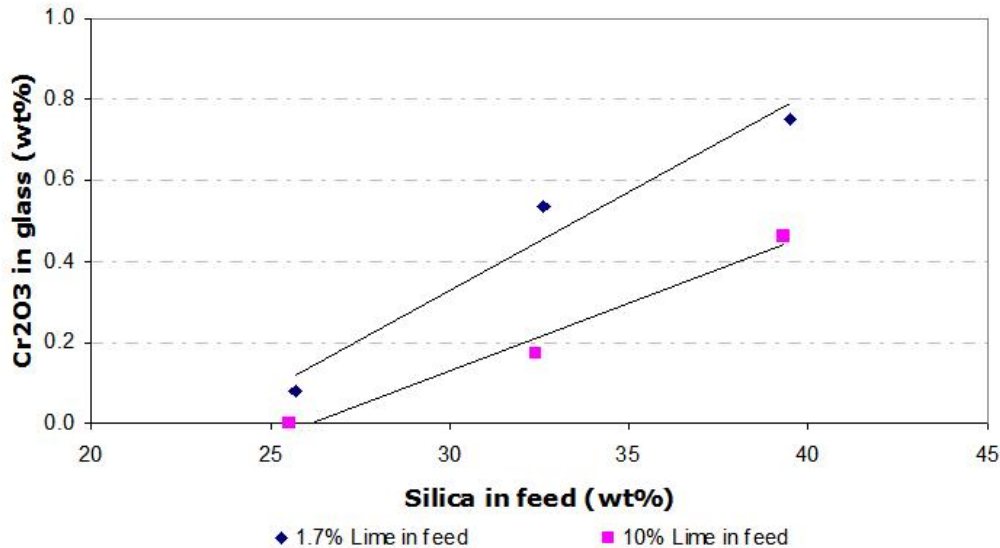
Figure 5.5 shows the amount of chrome reporting to the matte phase versus the amount of lime in the feed stream. In this figure the chrome is reported as Cr and not Cr_2O_3 which corresponds to the FactSage format of reporting chrome in the matte phase. From the figure an increase in lime increases the amount of chrome in the matte phase for both silica levels of 33%wt and 39%wt.

To conclude, increasing lime concentration in the feed decreases the amount of "liquid" chrome in the glass phase (present as $Cr(II)O$ and $Cr_2(III)O_3$) and increases the amount of chromium in the spinel phase as well as the matte phase.

5.3 The effect of the silica content of the feed stream on chrome deportment

The same experimental conditions discussed in section 5.2 were used to investigate the effect of silica on chrome deportment. Regarding the slag chemistry: the silica levels were varied at two lime set points while the other slag additives were kept constant.

Figure 5.6 shows a direct relationship between the amount of silica in the in the starting materials and the amount of chrome in the glass phase. The relationship is the same at both lime concentrations but at higher lime addi-

Figure 5.6: The relationship between the silica in feed stream and the chrome content of the glass phase

tions less chrome is dissolved into the glass phase. The figure shows that as the silica increases the amount of chrome that dissolved into the glass phase increased by 16%wt.

From figure 5.7 it can be seen that the amount of chromium in the spinel phases starts at 5.3%wt at 33%wt silica and decrease to almost zero at 39%wt silica (for the 10%wt lime system). The trend is true for both of the lime additions (1.7%wt and 10%wt).

Figure 5.8 shows the relationship between the concentration silica in the starting materials and the amount of chromium in the matte phase. At 33%wt silica the chrome content of the matte phase is 0.03%wt and increases to 0.05%wt at a silica and lime content of 39%wt and 1.7%wt respectivly.

The effect of silica can be summarized as follows: as the amount of silica in the feed stream is increased the amount of chromium dissolving into the glass phase increases. This is most likely due to the increasing amount of attachment sites created for the chromium ion on the silica structure (refer to section 2.3.1 and section 2.4.3). As for the spinel and matte phase, it seems that the chromium ion is exchanging between these two phases and the exchange ratio is dependent on the amount of silica in the feed stream.
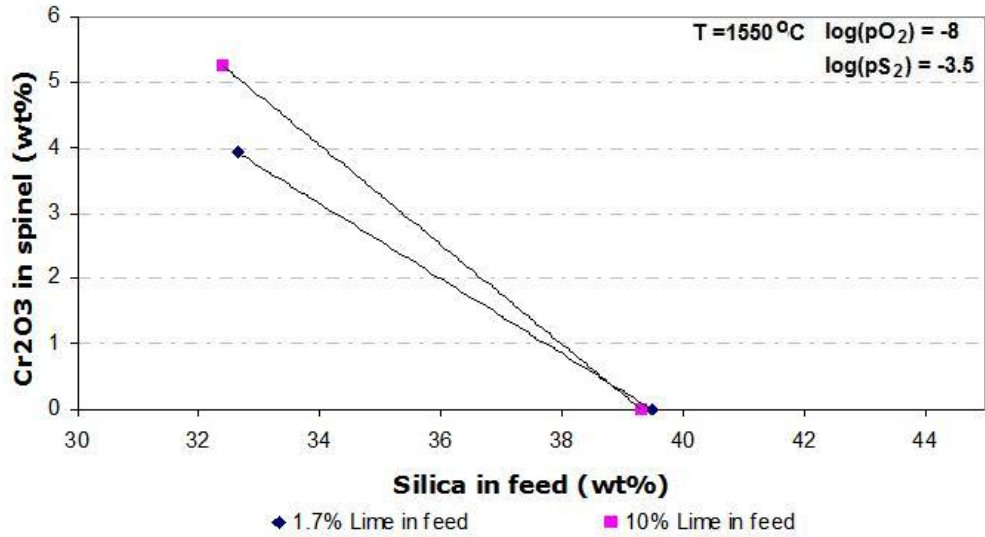
Figure 5.7: The relationship between the silica in feed stream and the chrome content of the spinel phase
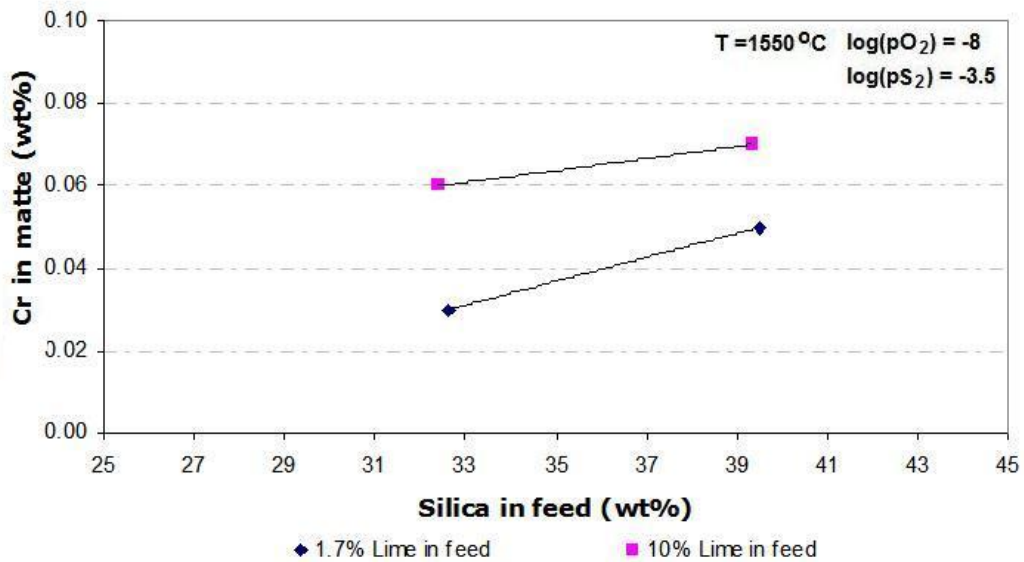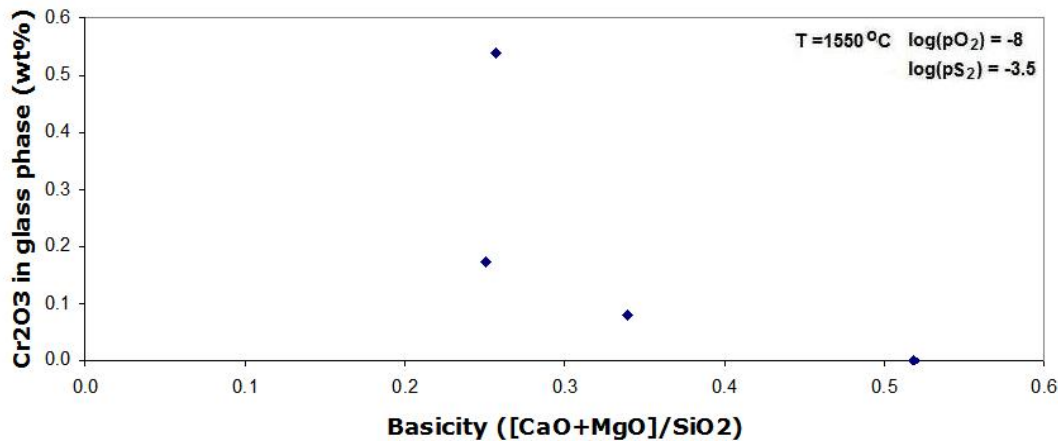

Figure 5.8: The relationship between the silica in the feed stream and the chrome content of the matte phase

Figure 5.9: The relationship between basicity and the chrome content of the glass phase

## 5.4 Basicity of glass phase and chrome deportment

This section covers the relationship between basicity and the chrome deportment between the matte and bulk slag phases. For comparison purposes a V3 basicity (calculated by adding lime magnesia and dividing the answer by the amount silica) was utilized. The values used to calculate basicity was taken from the product (glass phase that formed) and not the feed although they gave very simular trends.

The relationship between the basicity and the chrome content of the glass phase shows a trend very similar to the one discussed by Nell(refer to section 2.4.2) [7]. The trend indicates that the higher the basicity (more lime or magnesia or less silica) the less chrome will report to the glass phase (see figure 5.9).

Looking at the matte phase, figure 5.10 indicates that an increase in the basicity results in a direct increase in the amount chromium in the matte phase.

5.5 The effect of the alumina crucible dissolving into the slag sample

As explained in section 4.2 and section 4.6, the crucible containing the sample is continously dissolving into the slag phase. This section will discuss the hypothesis that although the alumina may have influenced the concentration of chrome in the different phases it did not have a significant effect on the
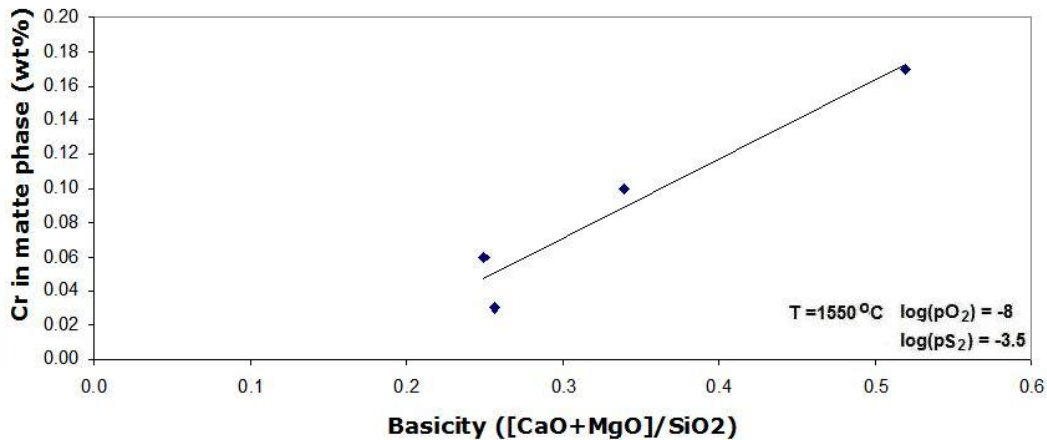
Figure 5.10: The relationship between basicity and the chrome content of the matte phase

trends discussed in sections 5.1, 5.2 and 5.3.

Figure 5.11 shows the amount of alumina in the glass phase versus the amount of lime in the feed. In the figure the alumina content of the glass phase varies as a function of lime content as well as silica content. The alumina content of the glass phase is between 33%wt and 39%wt depending on the lime and silica content. Considering the small change in alumina content of the glass phase it possible to say that the trends seen in figure 5.3 is not influenced by the additional alumina.

The effect of additional alumina on the silica versus chrome deportment trend is investigated in figure 5.12. In figure 5.12 the amount of alumina in the glass phase increases as the amount of silica in the feed stream increases. This is true for both lime concentrations. This effect of silica on alumina could mean that the trends seen in figure 5.6 could be as a result of the additional alumina in the glass phase. However, it has been found that additional alumina in the feed decreases the amount of chrome deporting to the glass phase (an 15%wt increase in alumina decreased the chrome content in the glass phase by 1.5%wt as discussed in section 2.4.2) [19]. Considering the research by Mintek it can be concluded that the trend seen in figure 5.6 is valid.

The last scenario that needs to be investigated is the effect of alumina on the amount of chrome in the matte phase. Figure 6.11 in Appendix (III) shows a scatter plot between the amount of chrome in the matte phase and the average amount of alumina in the slag phase. From the figure it is evident that there is no defenite relationship between these two components.
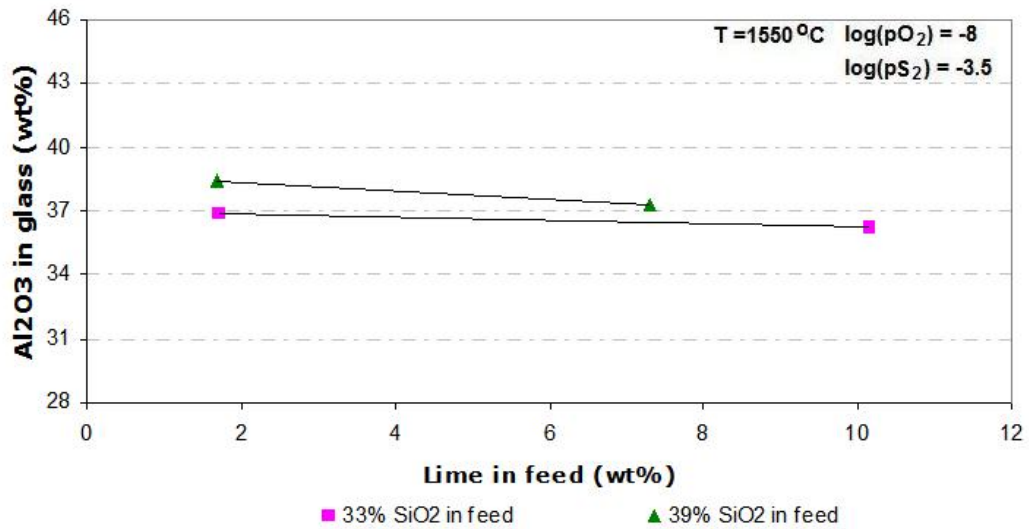
Figure 5.11: The amount of alumina in the glass phase versus the amount of lime in the feed.
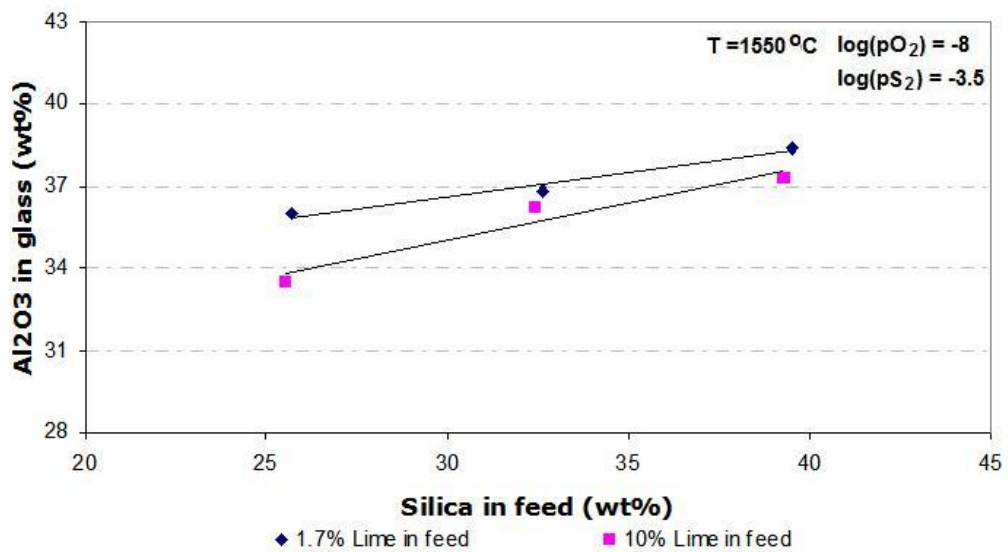
Figure 5.12: The amount of alumina in the glass phase versus the amount of silica in the feed.

Chapter 6

FactSage Validation

FactSage^{TM} uses thermodynamic properties to make predictions regarding the phases present in a specific system and the quantities of those phases (refer to section 2.5). Before FactSage^{TM} can be used in making predictions regarding the slag-matte system it is necessary to establish the integrity of the results obtained by FactSage^{TM}.

6.1 The effect of increasing the chrome content of the feed stream on chrome deportment

The following three figures shows the predicted effect of additional chromium in the feed stream on the chrome deportment in the system for the glass phase, spinel phase and matte phase respectively. Figure 6.1 shows the amount of dissolved chromium in the glass phase versus the amount of chromium oxide fed as predicted by FacSage^{TM}. Experimental trends observed in section 5.1 are also shown for comparison. From the figure it can be seen that the amount of dissolved chromium oxide in the slag phase remained at 0.9%wt when the amount of chromium oxide in the feed is varied between 1%wt and 3.5%wt. From the experimental results we see that the dissolved chrome in the glass phase did not remain constant but increased from 0.1%wt to 0.5%wt when the amount of chromium oxide in the feed is varied between 1%wt and 3.5%wt. This indicates that FactSage^{TM} over-predicted the chromium oxide levels in the glass phase for the different levels of chromium oxide fed.

Figure 6.2 shows the amount of chromium oxide reporting to the spinel phase as predicted by FactSage^{TM} as well as the experimental trends observed in section 5.1. The figure indicates that an increase in the amount of chromium oxide in the feed resulted in a direct increase of chromium oxide reporting to the spinel phase for both the predicted and experimental results. For the
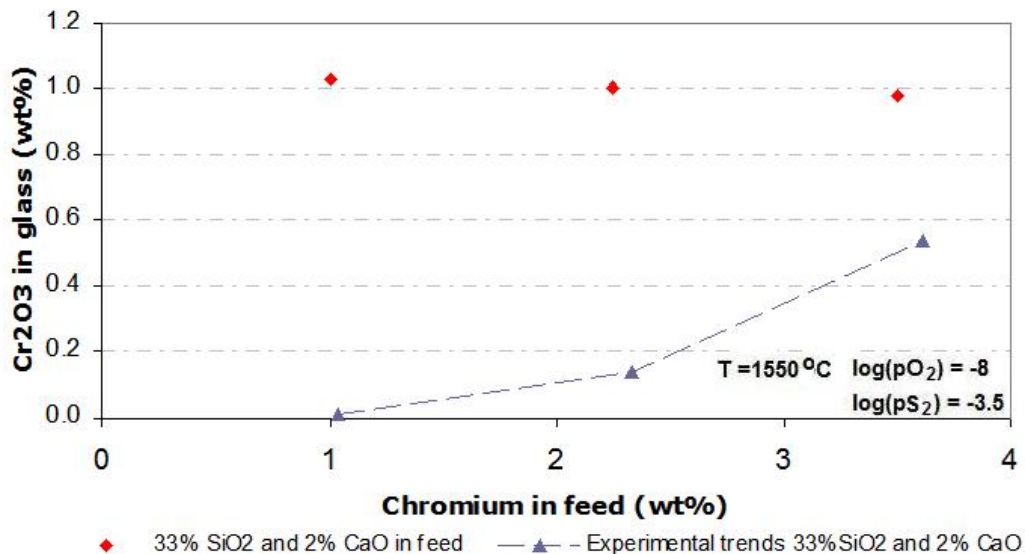
Figure 6.1: FactSage^{TM} results on the chromium oxide reporting to the glass phase versus chromium oxide fed

predicted results it can be noted that the gradient is smaller than that of the experimental results. This indicates that FactSage^{TM}, in this case, under-predicted the results.

Figure 6.3 indicates that the amount of chrome in the matte phase increases as the amount of chromium oxide in the feed stream increases. However, the amount of chromium oxide dissolved in the matte phase is 0.025%wt when the amount of chromium oxide fed is 1%wt. This amount is almost insignificant and increases to only 0.028%wt when the amount of chromium oxide fed is equal to 3.5%wt. Even though the predicted values obtained are small they do compare with the actual experimental values on the same figure. The low weight percentages of chromium oxide in the matte phase indicates that chromium oxide has a low solubility in this phase.
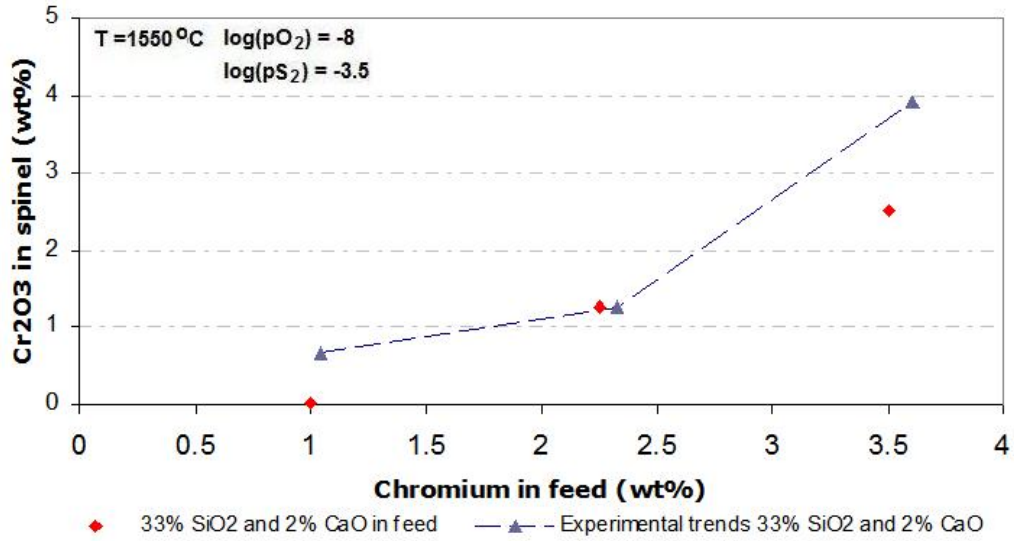
Figure 6.2: FactSage^{TM} results on the chromium oxide reporting to the spinel phase versus chromium oxide fed
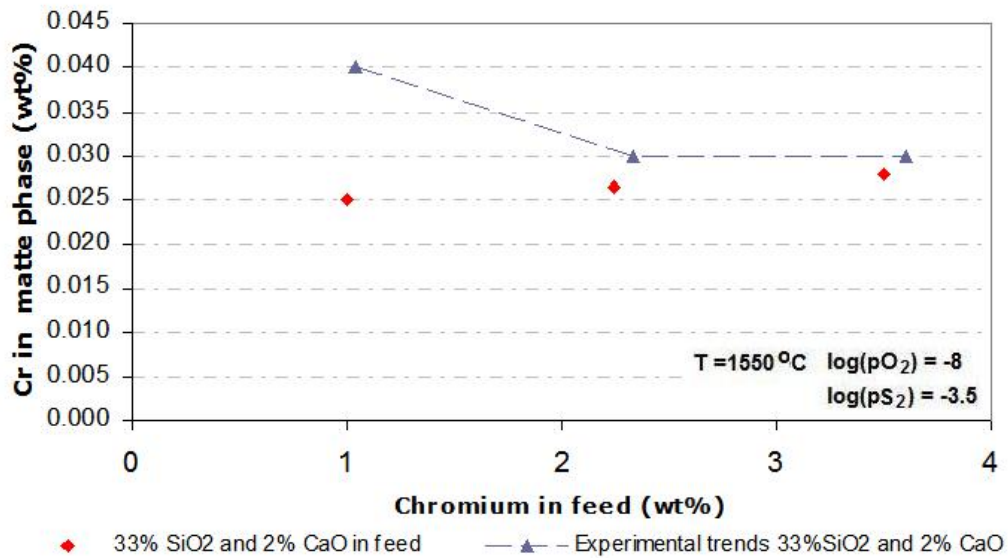

Figure 6.3: FactSage^{TM} results on the chromium oxide dissolved into the matte phase versus chromium oxide fed

6.2 The effect of increasing the lime content of the feed stream on chrome deportment

Figure 6.4 shows the relationship between the lime fed and the amount of Cr_2O_3 in the glass phase. The figure shows that as the lime increases the amount of Cr_2O_3 in the glass phase decreases. A 10%wt increase in lime decreases the amount of Cr_2O_3 in the glass by 0.4%wt for the 39%wt SiO_2 system. For the 33%wt SiO_2 system the same trend is observed (6%wt increase in lime fed decreases the amount of Cr_2O_3 in the glass phase by 0.3%wt). This indicates that at higher silica levels the effect of additional lime (lowering the amount of chromium oxide in the glass phase) is more severe.

The experimental trends that were obtained in section 5.2 forms the same trend as the predicted results. However, the experimental results shows lower chromium oxide contents in the glass phase. FactSage^{TM} therefore over-predicts the chrome content of the glass phase. This was also seen in section 6.1 were FactSage^{TM} over predicted the amount of chromium oxide reporting to the glass phase as a function of the amount of chromium oxide fed.

Figure 6.5 shows the effect of increasing the lime content of the feed stream on the amount of Cr_2O_3 reporting to the spinel phase. From the figure the amount of chrome reporting to the spinel phase increases as the amount of lime increases. For the 33%wt SiO_2 system an 10%wt increase in lime increased the amount of chrome reporting to the spinel phase by 0.3%wt. The same trend is seen for the 39%wt SiO_2 system at a lime increase of 6%wt.

The experimental trend shows an identical pattern but indicates that the effect of additional lime is more severe. From the experimental results a 10%wt increase in lime increased the chrome content of the spinel phase by 1.2%wt.

The FactSage^{TM} prediction in figure 6.6 indicates that additional lime in the feed stream would lower the amount of chrome in the matte phase. For practical purposes it can be seen as staying relatively constant. In this figure the trends formed from experimental values are showing a different result. Here, as was discussed previously, an increase in lime increases the amount of chrome in the matte phase.
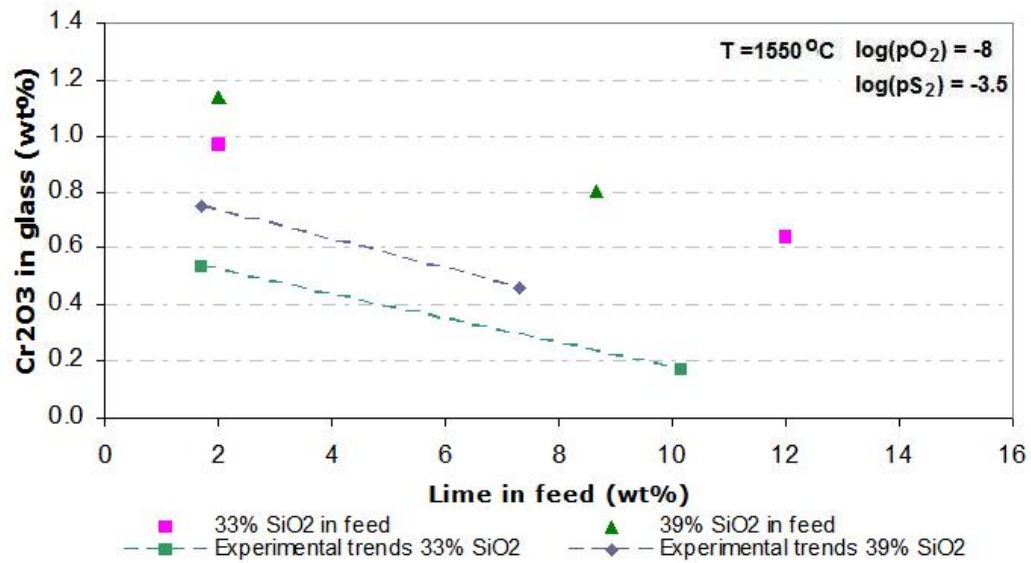
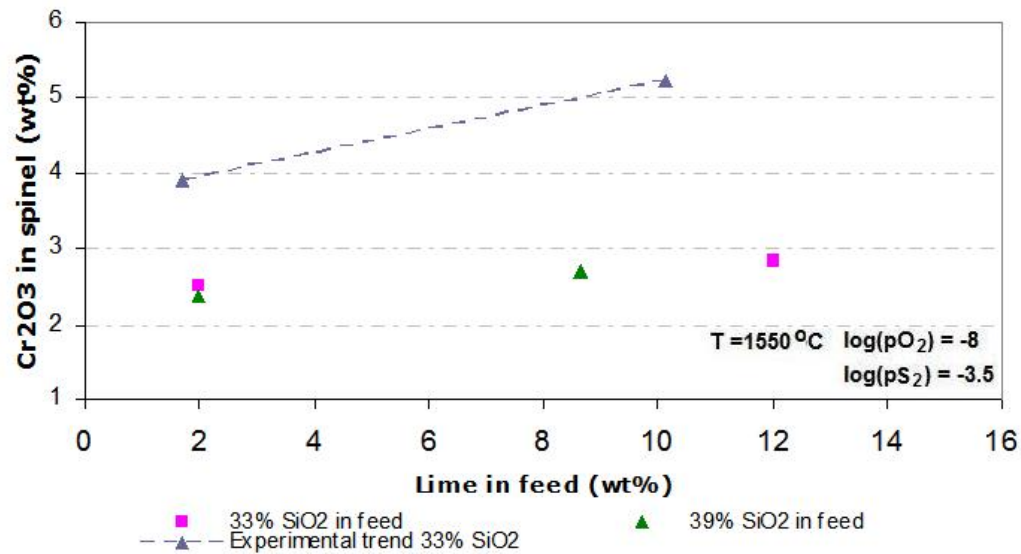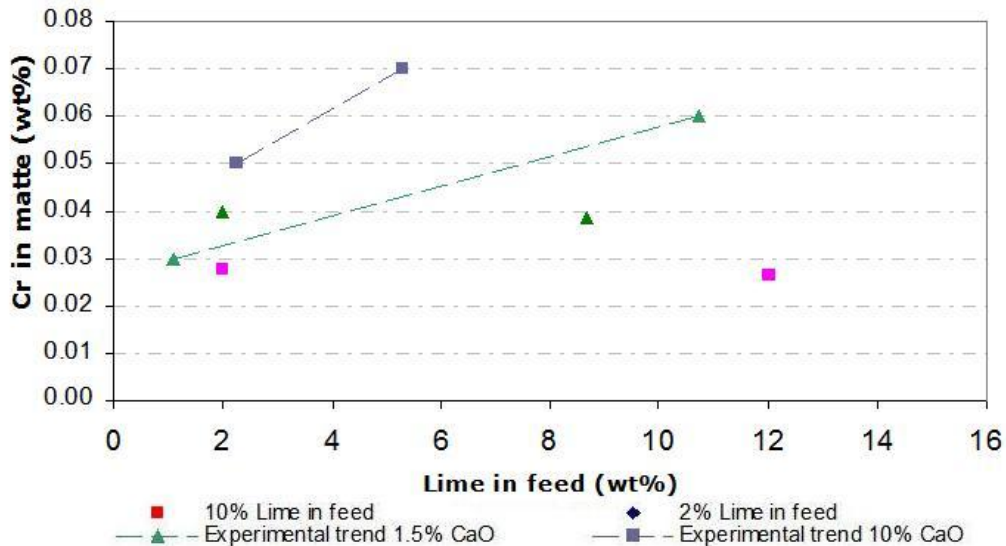**Figure 6.4:** FactSage^{TM} results on the effect of lime additions in feed versus Cr_2O_3 wt% in the glass phase

Figure 6.5: FactSage^{TM} results on the effect of lime additions in feed versus Cr_2O_3 wt% in the spinel phase
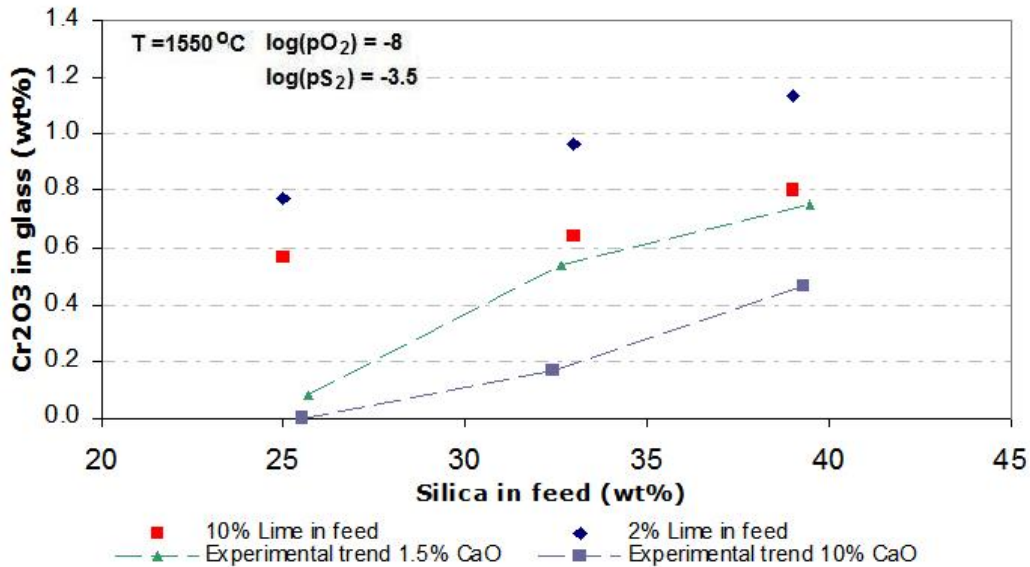
Figure 6.6: FactSage^{TM} results on the effect of lime additions in feed versus Chrome content of matte phase

6.3 The effect of increasing the silica content of the feed stream on chrome deportment

The effect of increasing the amount of silica in the feed stream on the amount of chrome in the glass phase can be seen in figure 6.7. This figure indicates that as more silica is added to the system more chrome reports to the glass phase. For a 10%wt lime system, an increase of 15%wt in silica resulted in an increase of 0.25%wt in chromium oxide reporting to the glass phase. The silica effect is more severe for the low lime system (1.5%wt) where an increase of 15%wt silica increased the amount of chromium oxide that is dissolved in the glass phase by 0.35%wt.

The trends observed for the experimental results are similar but the effect of silica is greater. For the 10%wt lime system a 20%wt increase in silica increased the amount of chromium oxide in the glass phase by 0.46%wt. For the 1.5%wt lime system the chromium oxide increased with only 0.67%wt. From this figure it can also be seen that FactSage^{TM}, once again, over predicted the chrome content of the glass phase.

FactSage^{TM} indicates that additional silica in the feed does not affect the chrome content of the spinel phase significantly (refer to figure 6.8). For the 10%wt lime system an increase of 15%wt silica decreased the chrome content of the spinel phase by 0.3%wt compared to 0.4%wt for the 1.5%wt lime system. The experimental trends plotted on the same figure shows similar trends but affects the chrome deportment in a whole different degree. For the exper-
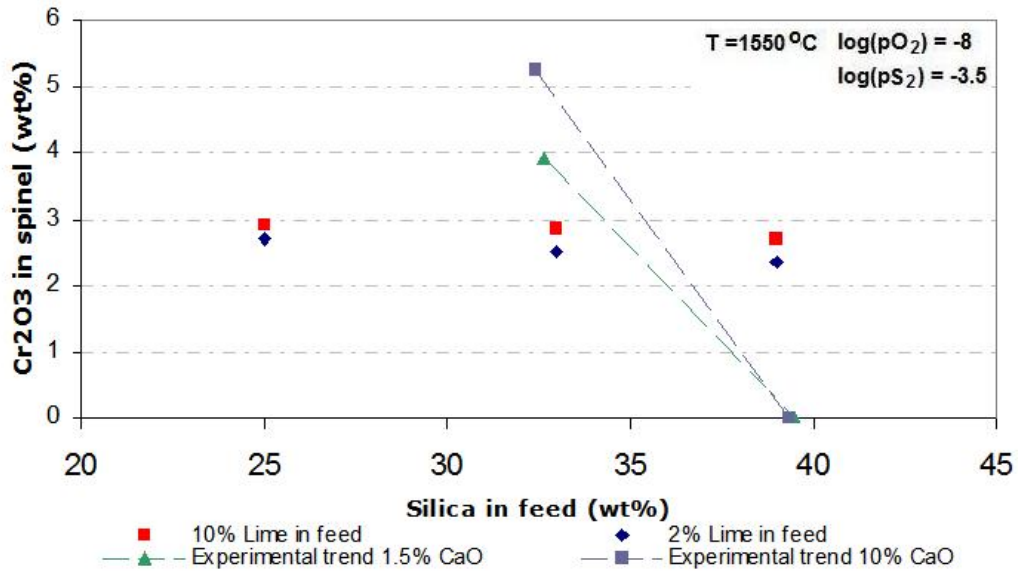
Figure 6.7: FactSage^{TM} results on the effect of silica additions in feed versus Cr_2O_3 wt% in the glass phase

imental trends (1.5%wt lime system) a 6%wt increase decreased the chrome content of the spinel phase from 6%wt down to 0%.

The last prediction shows the effect of additional silica on the chrome content of the matte phase. Figure 6.9 illustrates this effect. The first point to note is that the concentration of chromium oxide in the matte phase is very low (averaging between 0.02%wt and 0.07%wt). Secondly, the figure indicates that the chrome content of the matte phase increases with the amount of silica in the feed stream. For 15%wt increase in silica the chrome content of the matte phase increases from 0.016%wt to 0.039%wt and is relatively similar for both the 1.5%wt and the 10%wt lime system.

When the experimental trends are compared the same effect of silica on the chrome content of the matte phase is observed. The 1.5%wt lime system compares well to the values obtained with the FactSage^{TM} predictions. The experimental values obtained for the 10%wt lime system, however, shows significant more chrome in the matte phase. FactSage^{TM} therefore under-predicted the chrome content of the matte phase.

Hence FactSage^{TM} consistently over-predicts the chrome deportment to the glass phase and the spinel phase and under-predicts the chrome deportment to the matte phase.

Figure 6.8: FactSage^{TM} results on the effect of silica additions in feed versus Cr_2O_3 wt% in the spinel phase
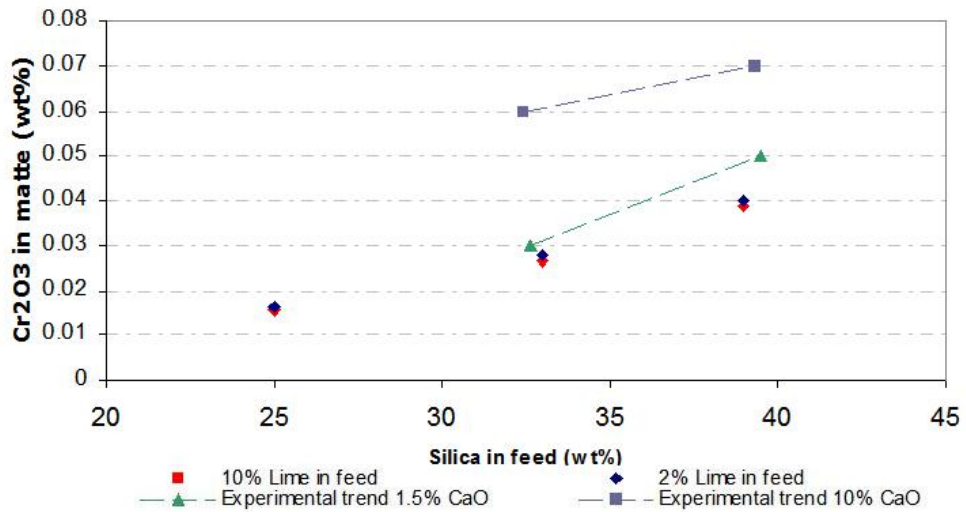
Figure 6.9: FactSage^{TM} results on the effect of silica additions in feed versus chrome content of the matte phase

Conclusions

The conclusions that was drawn from the results will be discussed in line with the hypothesis and objectives set out for this project. These conclusions are:

1. Section 4.2 concludes that there is no material that would be inert to the system that was investigated in this project and that the crucible used will, to some extent, interfere with the resutls obtained.

2. From section 4.6 it is evident that the system is not in complete equilibrium due to the alumina crucible disolving into the slag sample. In order to counter this phenomna, a reaction time was chosen to give the slag and matte phase enough time to interact but not enough time for the crucible to loose its structural integrity.

3. From section 5.1 the chrome content of the slag phase and spinel phase are directly related to the amount of chrome fed. Experiemental results showed that increasing the chrome content of the starting materials increases the chrome content of the glass phase as well as the spinel phase.

4. In section 5.2 it is clear that an increase in lime content of the feed increases the amount of chrome in the spinel phase and matte phase. This means that the chrome content of the liquid slag phase decreases when the amount of lime in the feed is increased.

5. Section 5.3 shows that more chrome is disolved into the liquid slag phase when the silica content of the feed is increased.

6. In section 5.4 it is shown that chrome deportment is a function of not only lime and silica but also the interaction between these oxide species. The results obtained from the plot shows that an increase in basicity decreases the amount of chrome deporting to the slag phase. This section also indicated that there is a direct relationship between basicity and the amount of chrome deporting to the matte phase.

7. From section 5.5 it was concluded that alumina did have a dilution effect on the system but that it did not influence the trends (increase or decrease) that were observed.

8. In section 6 it was seen that FactSage^{TM} is able to predict the effect of certain slag additives on chrome deprotment however, FactSageTM overpredicts the amount of chrome reporting to the slag phase.

Recommendations

Based on the conclusions the following recommendations were made:

1. **Lime additions.** Out of a chrome deportment point of view lime addtions in the PGM industry should be reduced to reduce chrome deportment to the spinel phase ensuring less solid formation during furnace opeartion.

2. **FactSage^{TM} validations.** FactSage^{TM} validations should be extended to temperature and partial pressures as these are critical factors in the smelting industry.

3. **Further studies.** Only a few of the parameters were investigated in this research project due to time limitations. Other parameters that still needs investigation are changes in partial pressure and temperature.

4. **Investigation into the use of zirconia crucibles.** Investigation is neccesary into the use of high quality dense zirconia crucibles as a more inert material than the alumina crucible that was used in this study.

Appendix I: Possible Sources of Errors

1. Weighing Errors. A taurus electronic scale was used for all weighing purposes. The scale meassures the fourth decimal making it accurate to the third decimal. Weighing errors could have occured during the prepation of the master slags and during the addition of the sulphides just before the sample was suspended in the furnace. The master slags were prepared in batches of 15 grams to restrict the error to 0.5%. Unforunatly the sulphides could not be added in such large quantities which made room for a possible error of 0.8%.

2. Temperature Flucuations. Due to the design of the tube furnace the temperature inside the furnace flucuates with 5^oC from the furnace set point. This flucuations adds up to an experimental error of 0.3%.

3. Material Contamination. All precautions were taken to prevent any contaminations from unwanted materials however, it was found that a part of the crucibles used to contain the material in the tube furnace disovled into the slag.

4. Partial Pressures. There are two sources of errors when trying to maintain the correct partial pressure inside the tube furnace. These include an error in the FactSage predictions (model) and secondly during the measurements of the gasflow rates injected into the furnace. After investigation it was seen that there was an error but that the partial pressure and the predicted partial pressure was in the same magnitude. The error was acceptable for this reseach project due to the difficulty of meassuring the actual partial pressure inside a real platinum producing furnace.

Appendix II: Additional results
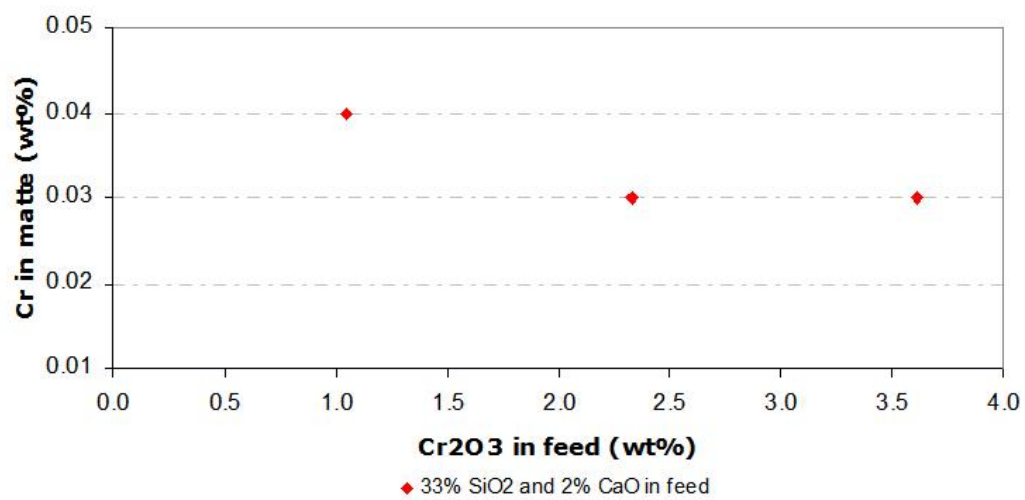
Figure 6.10: The chrome content of the matte phase versus the amount of chromium oxide fed
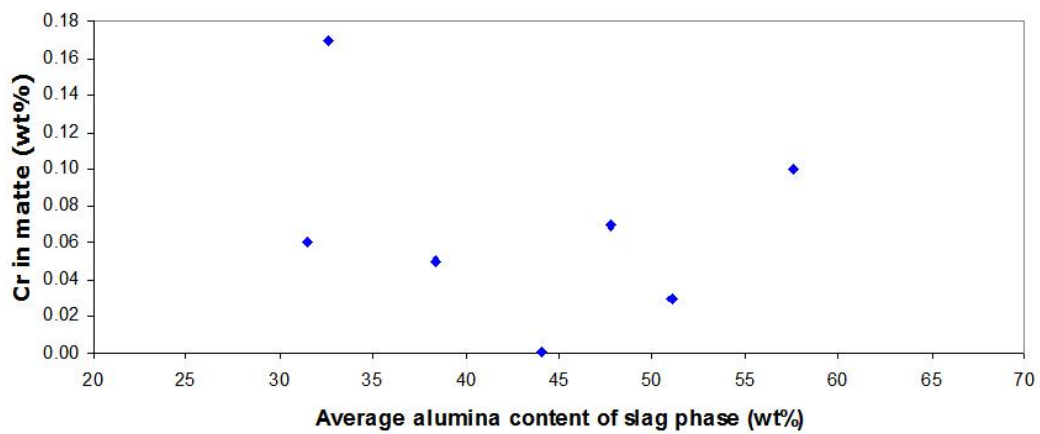
Figure 6.11: The amount of alumina in the slag phase versus the amount of chrome in the matte phase.

Appendix III: Feed compositions, slag analysis and matte analysis

Sample no:3

Feed Compositions

Cr2O3	CaO	SiO2	MgO	Al2O3	Fe	Ni	Cu	S
3	1.7	26	18.3	18	18.6	3	1.9	6.9

Slag Analysis

Phase no:	Cr2O3	Fe2O3	NiO	CuO	MgO	Al2O3	SiO2	CaO
Average	0.6	24.3	0.3	0.1	9.7	57.6	9.4	1.4
4	0.08	21.6	0	0	4.1	36	33.9	7.4
5	0.06	20.4	0.1	0	8.1	68.3	0.3	0
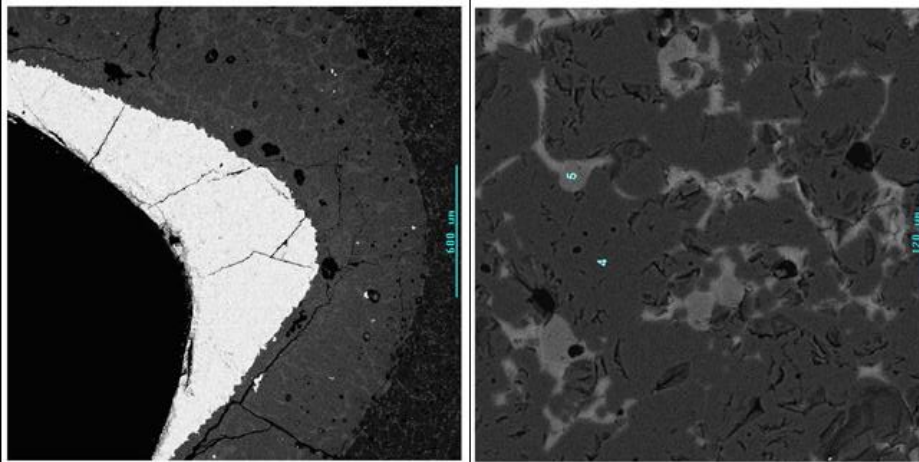
Figure 6.12: The feed and slag analysis of sample no.3

Sample no:3

Matte Analysis

Phase no:	Cr	Fe	Ni	Cu	S
Average	0.02	32.7	61.4	5.6	1.4
Phase no:	Cr	Fe	Ni	Cu	S
1	0.02	32.7	61.4	5.6	1.4
Phase no:	Cr	Fe	Ni	Cu	S
2	0.08	13.5	7.4	57.7	23.6
Phase no:	Cr	Fe	Ni	Cu	S
3	0.04	32.6	34	2.3	32.8
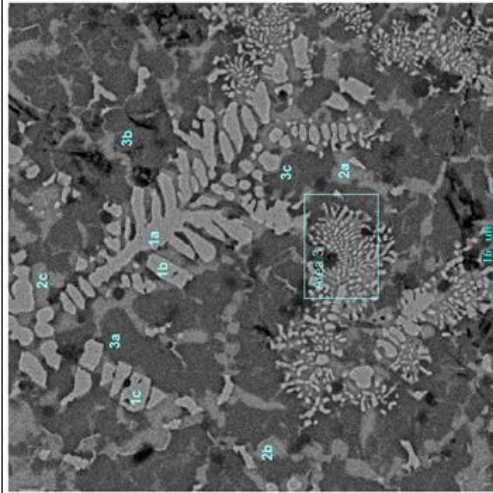
Figure 6.13: The matte analysis for sample no.3
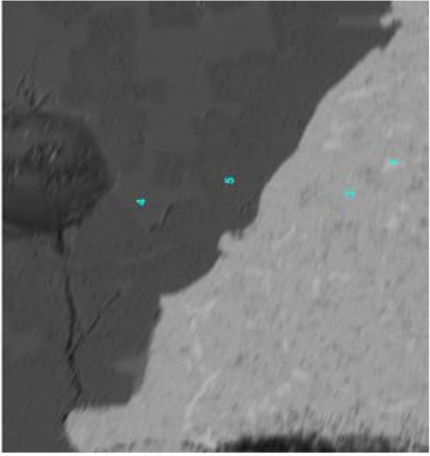
Sample no:12

Feed Compositions

Cr2O3	CaO	SiO2	MgO	Al2O3	Fe	Ni	Cu	S
3	10.2	26	15	18	16	2.5	1.6	5.7

Slag Analysis

Phase no:	Cr2O3	Fe2O3	NiO	CuO	MgO	Al2O3	SiO2	CaO
Average	0.08	15	0.02	0.13	4.5	33	32	13
Phase no:	Cr2O3	Fe2O3	NiO	CuO	MgO	Al2O3	SiO2	CaO
4	0.49	15.6	0	0	14.8	62	0.47	0
Phase no:	Cr2O3	Fe2O3	NiO	CuO	MgO	Al2O3	SiO2	CaO
5	0	13.4	0	0	4.6	33.5	33	12.6

Figure 6.14: The feed and slag analysis of sample no.12

Sample no:12

Matte Analysis

Phase no:	Cr	Fe	Ni	Cu	S
Average	0.04	38	20	20	23
Phase no:	Cr	Fe	Ni	Cu	S
1	0	42.1	44.5	8.8	4.4
Phase no:	Cr	Fe	Ni	Cu	S
2	0.108	47	18.2	11	22.4
Phase no:	Cr	Fe	Ni	Cu	S
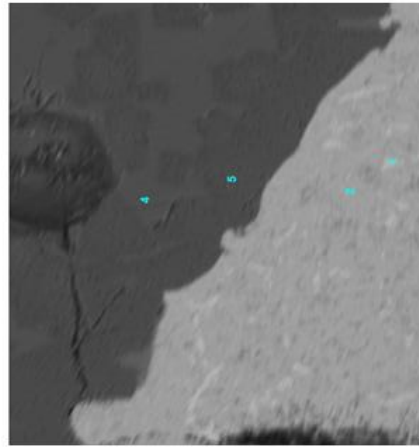
Figure 6.15: The matte analysis for sample no.12

Sample no:13

Feed Compositions

Cr2O3	CaO	SiO2	MgO	Al2O3	Fe	Ni	Cu	S
0.85	1.7	32.7	16.6	18	16.8	2.7	1.7	6.3

Slag Analysis

Phase no:	Cr2O3	Fe2O3	NiO	CuO	MgO	Al2O3	SiO2	CaO
Average	0.4	15.3	0.4	0.	11.4	63	11.3	0.6
4	0.01	18.5	0.3	0.2	7.6	37.5	37.4	2
5	0.67	14.9	1	0	13.9	73.6	0.3	0
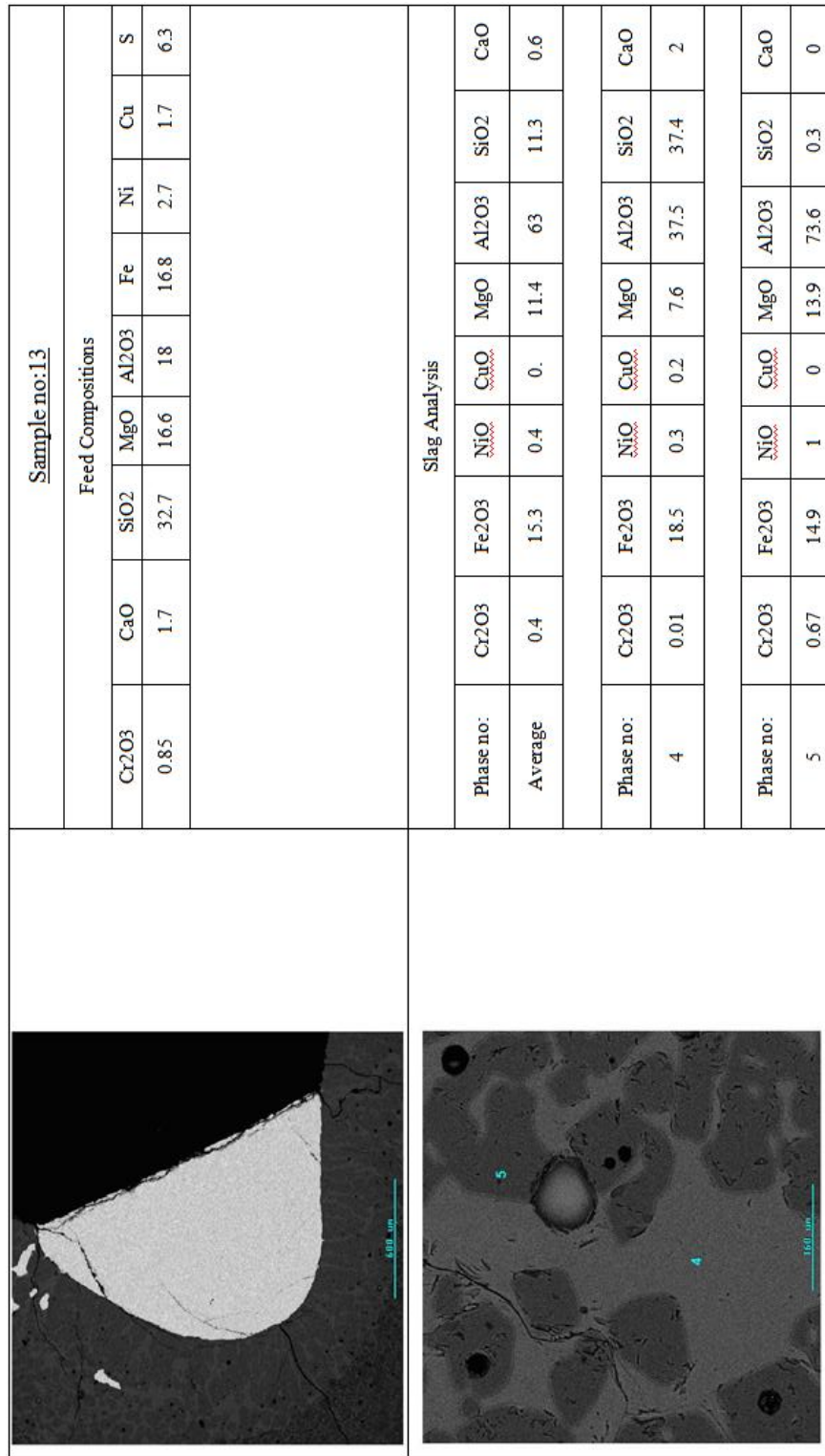
Figure 6.16: The feed and slag analysis of sample no.13

Sample no:13

Matte Analysis

Phase no:	Cr	Fe	Ni	Cu	S
Average	0	15	46	22	19
Phase no:	Cr	Fe	Ni	Cu	S
1	0.02	21	70	9.7	0.71
Phase no:	Cr	Fe	Ni	Cu	S
2	0.09	8.3	5	64	23
Phase no:	Cr	Fe	Ni	Cu	S
3	0.02	14	56	3.4	28
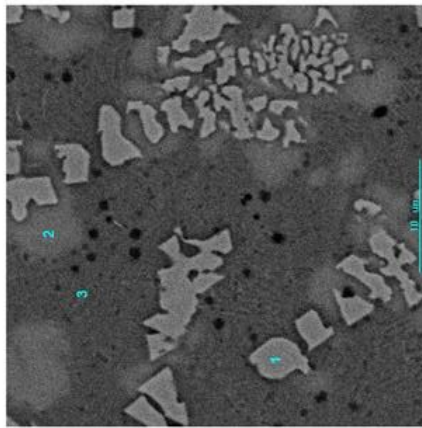
Figure 6.17: The matte analysis for sample no.13

Sample no:14

Feed Compositions

Cr2O3	CaO	SiO2	MgO	Al2O3	Fe	Ni	Cu	S
1.9	1.7	33	16	18	16	2.6	1.7	6.1

Slag Analysis

Phase no:	Cr2O3	Fe2O3	NiO	CuO	MgO	Al2O3	SiO2	CaO
Average	1.1	11	1.1	0.3	12	67	11	0.5
4	0.14	14	0	0.3	8.2	37	42	2.3
5	1.26	10.3	1.6	0	15	76	0.2	0.1

Figure 6.18: The feed and slag analysis of sample no.14

Sample no:14

Matte Analysis

Phase no:	Cr	Fe	Ni	Cu	S
Average	0	10	67	7.8	16.6
Phase no:	Cr	Fe	Ni	Cu	S
1	0.05	16	80	5.7	0.1
Phase no:	Cr	Fe	Ni	Cu	S
2	0.03	5.9	30.6	41	24
Phase no:	Cr	Fe	Ni	Cu	S
3	O	7.5	64	2	27
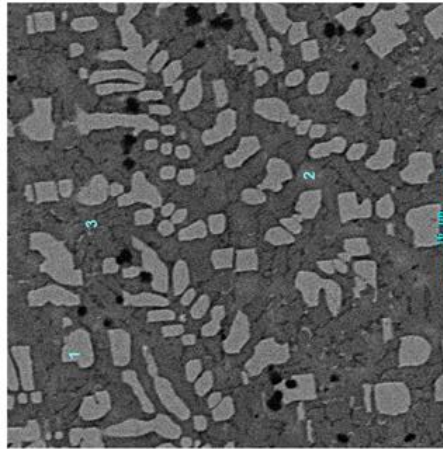
Figure 6.19: The matte analysis for sample no.14
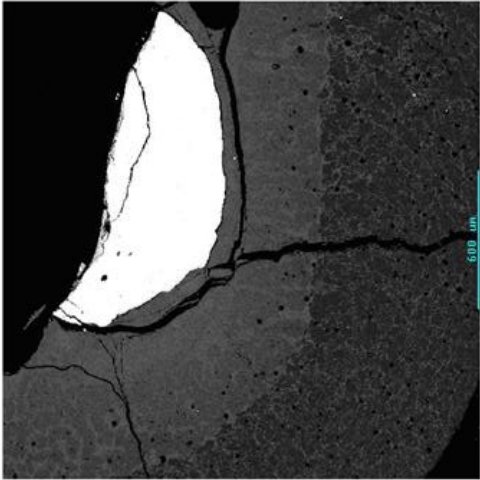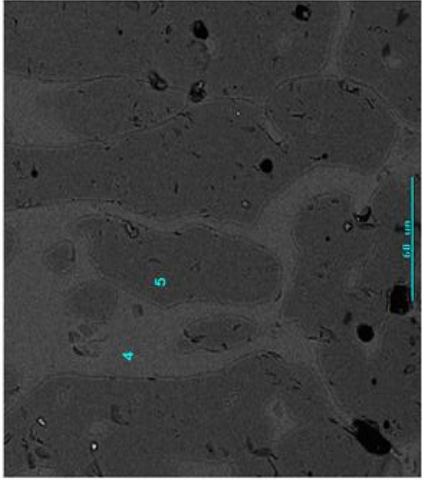
Sample no:15

Feed Compositions

Cr2O3	CaO	SiO2	MgO	Al2O3	Fe	Ni	Cu	S
3	1.7	33	16	18	16	2.6	1.6	5.9

Slag Analysis

Phase no:	Cr2O3	Fe2O3	NiO	CuO	MgO	Al2O3	SiO2	CaO
Average	2.3	15	0.7	0.2	12	51	21	1.1
Phase no: 4	0.14	14	0	0.3	8.2	37	42	2.3
Phase no: 5	1.3	10	1.6	0	15	76	0.2	0.1

Figure 6.20: The feed and slag analysis of sample no.15

Sample no:15							
Matte Analysis							
Phase no:	Cr	Fe	Ni	Cu	S
Average	0.03	14	46	23	19
Phase no:	Cr	Fe	Ni	Cu	S
1	0.004	21	71	8.1	0.49
Phase no:	Cr	Fe	Ni	Cu	S
2	0.07	11	23	43	25
Phase no:	Cr	Fe	Ni	Cu	S
3	0.06	14	56	3.3	27
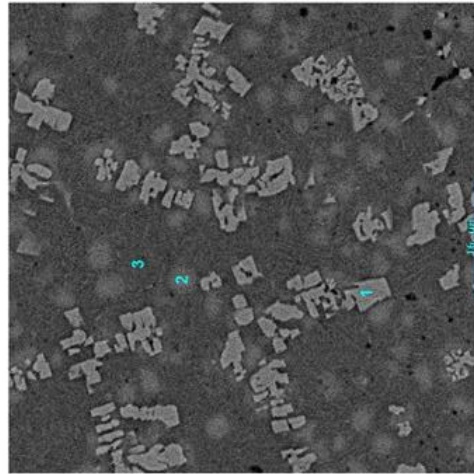
Figure 6.21: The matte analysis for sample no.15

Sample no:24

Feed Compositions

Cr2O3	CaO	SiO2	MgO	Al2O3	Fe	Ni	Cu	S
3	10	32	13	18	13	2.1	1.3	4.9

Slag Analysis

Phase no:	Cr2O3	Fe2O3	NiO	CuO	MgO	Al2O3	SiO2	CaO
Average	2.4	14	0.18	0.11	10	40	28	7.6

Phase no:	Cr2O3	Fe2O3	NiO	CuO	MgO	Al2O3	SiO2	CaO
4	0.6	13	0.1	0.2	7	33	38	11

Phase no:	Cr2O3	Fe2O3	NiO	CuO	MgO	Al2O3	SiO2	CaO
5	5.24	14	0.4	0	18	66	0.2	0.1
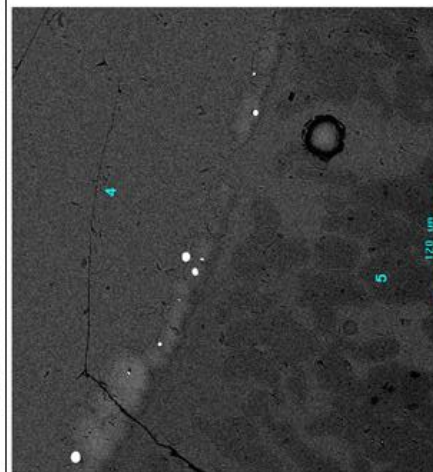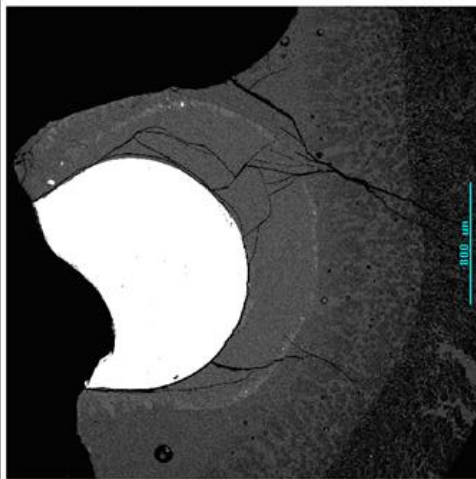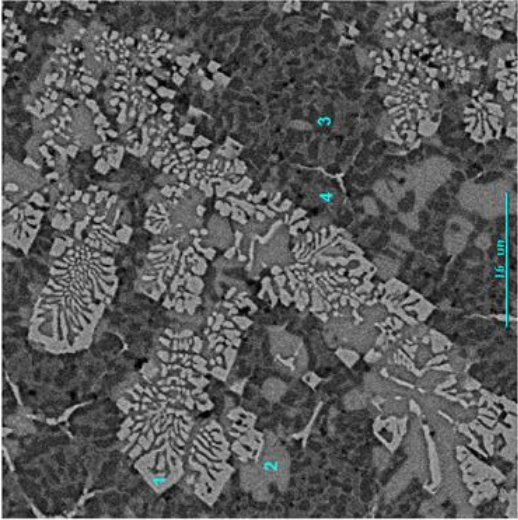
Figure 6.22: The feed and slag analysis of sample no.24

Sample no:24

Matte Analysis

Phase no:	Cr	Fe	Ni	Cu	S
Average	0.2	20	42	19.6	19.2
1	0.08	24	63	12	3.2
2	.001	7.4	2.3	69	23
3	.05	15	56	2.3	29

Figure 6.23: The matte analysis for sample no.24
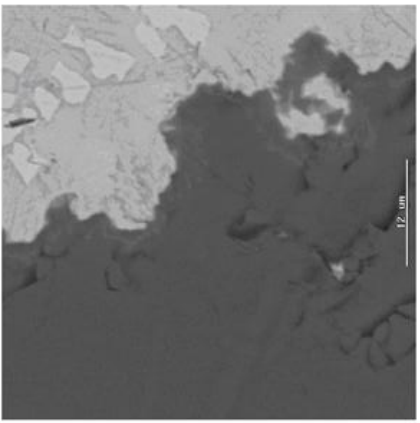
Sample no:27

Feed Compositions

Cr2O3	CaO	SiO2	MgO	Al2O3	Fe	Ni	Cu	S
3	1.7	40	13	18	14	2.2	1.4	5.1

Slag Analysis

Phase no:	Cr2O3	Fe2O3	NiO	CuO	MgO	Al2O3	SiO2	CaO
Average	0.91	1.5	0.08	0	6.9	34	37	2.3
Phase no:	Cr2O3	Fe2O3	NiO	CuO	MgO	Al2O3	SiO2	CaO
4	0.87	13.9	0.8	0	8.2	37.8	40.8	2.1
Phase no:	Cr2O3	Fe2O3	NiO	CuO	MgO	Al2O3	SiO2	CaO
5	0	0	0	0	0	0	0	0

Figure 6.24: The feed and slag analysis of sample no.27
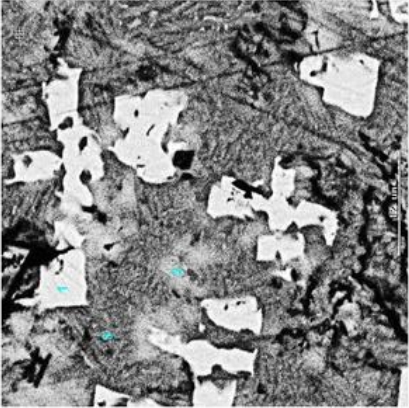
Sample no:27						
Matte Analysis						
Phase no:	Cr	Fe	Ni	Cu	S	
Average	0.04	8.4	57	13	21	
Phase no:	Cr	Fe	Ni	Cu	S	
1	0.05	15.33	71.76	10.4	0.83	
Phase no:	Cr	Fe	Ni	Cu	S	
2	0.03	5.7	14.3	55.3	23	
Phase no:	Cr	Fe	Ni	Cu	S	
3	0.04	8.53	60.57	3.3	25.9	

Figure 6.25: The matte analysis for sample no.27

Sample no:33

Feed Compositions

Cr2O3	CaO	SiO2	MgO	Al2O3	Fe	Ni	Cu	S
3	7.3	39	12	18	12	1.9	1.2	4.3

Slag Analysis

Phase no:	Cr2O3	Fe2O3	NiO	CuO	MgO	Al2O3	SiO2	CaO
Average	1	9.1	0.6	0.2	11	48	26	5.3
Phase no:	Cr2O3	Fe2O3	NiO	CuO	MgO	Al2O3	SiO2	CaO
4	1.6	9.1	0.3	0.4	7.7	36.4	37.7	10.7
Phase no:	Cr2O3	Fe2O3	NiO	CuO	MgO	Al2O3	SiO2	CaO
5	0	0	0	0	0	0	0	0
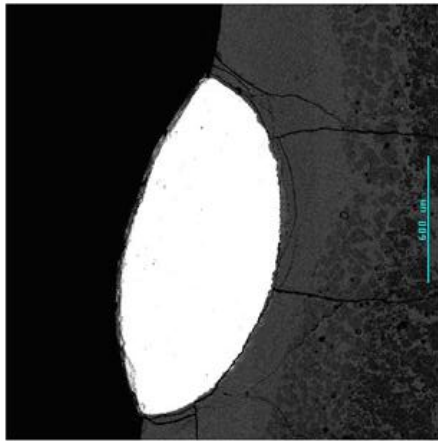
Figure 6.26: The feed and slag analysis of sample no.33

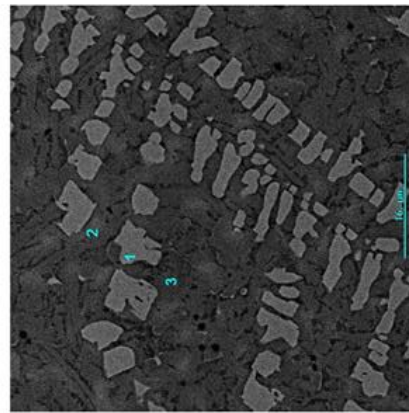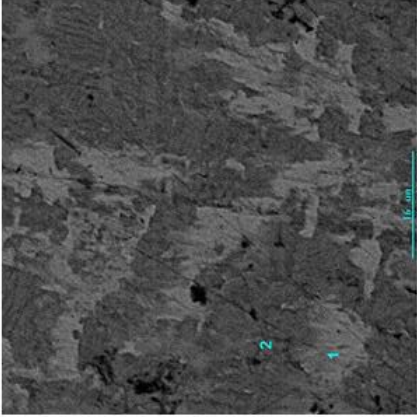| Sample no:33						
Matte Analysis						
Phase no:	Cr	Fe	Ni	Cu	S	
Average	0.08	9.6	59	9.5	22	
Phase no:	Cr	Fe	Ni	Cu	S	
1	0.01	16.8	77.7	6	0.12	
Phase no:	Cr	Fe	Ni	Cu	S	
2	0.1	7.1	21.9	48	24.2	
Phase no:	Cr	Fe	Ni	Cu	S	
3	0.08	8.8	59.8	4.8	27.1	

Figure 6.27: The matte analysis for sample no.33
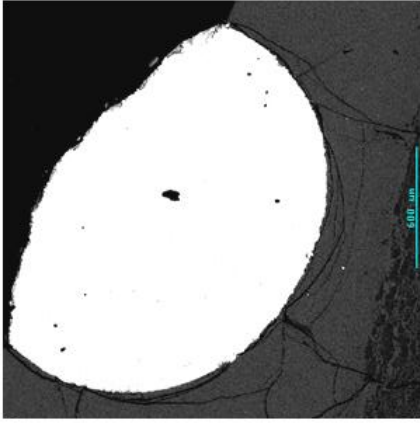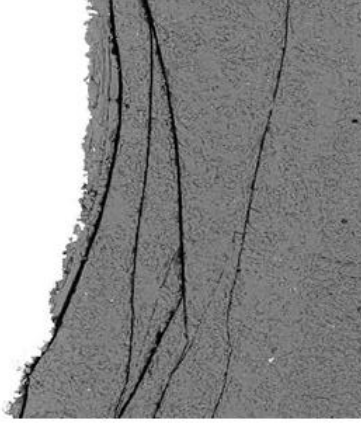
Sample no:39

Feed Compositions

Cr2O3	CaO	SiO2	MgO	Al2O3	Fe	Ni	Cu	S
2.95	1.68	46.3	11	18	11.2	1.8	1.14	4.16

Slag Analysis

Phase no:	Cr2O3	Fe2O3	NiO	CuO	MgO	Al2O3	SiO2	CaO
Average	3	11.7	0.4	0	11.1	44.1	29.4	1

Phase no:	Cr2O3	Fe2O3	NiO	CuO	MgO	Al2O3	SiO2	CaO
4	0	0	0	0	0	0	0	0

Phase no:	Cr2O3	Fe2O3	NiO	CuO	MgO	Al2O3	SiO2	CaO
5	0	0	0	0	0	0	0	0

Figure 6.28: The feed and slag analysis of sample no.39

Sample no:39

Matte Analysis

Phase no:	Cr	Fe	Ni	Cu	S
Average	0.001	9.7	54.6	14	20.4
Phase no: 1	0.01	14.72	62.2	18.7	3.9
Phase no: 2	0	5.9	67	2	27.1
Phase no:	Cr	Fe	Ni	Cu	S

Figure 6.29: The matte analysis for sample no.39

Nomenclature

amo   activity constant

G Standard free energy of formation [kj/mole]

K Equilibrium constant

P_{O_2} Partial pressure of oxygen [atm]

R Universal gas constant [j/mole.K]

T Temperature [K]

Bibliography

[1] R T Jones. An overview of south african pgm smelting. In *Nickel and Cobalt: Challenges in Extraction and Production, 44th Annual Conference of Metallurgists, Calgary, Alberta, Canada*, 2005.

[2] R G Cawthorn. The platinum and palladium resources of the bushveld complex. *South Africa Journal of Science*, 95:481–489, 1999.

[3] A R Barnes and A F Newall. Spinel removal from pgm smelting furnaces. In *South African Institute of Mining and Metallurgy, Johannesburg, 5-8 March*, 2006.

[4] J Davis. Personal communication, 2009.

[5] G E Davidson and G K Chunnet. Seismic exploration for merensky reef, the way forward. *South African Journal of Geology*, v.102:p.261–267, September 1999.

[6] R du Preez. Personal communication, 2009.

[7] J Nell. Melting of platinum group metal concentrates in south africa. *The South Africa institute of mining and metallurgy*, August:423 – 427, 2004.

[8] R T Jones. Jom world nonferrous smelter survey, part2: Platinum group metals. *Industrial Survey*, pages 59–63, 2004.

[9] R T Jones and I J Kotze. Dc arc smelting of difficult pgm-containing feed materials. *International Platinum Conference*, pages 33–36, 2004.

[10] Wei-kao lu Riboud P V , Nobuo Sano, editor. *Advanced Physical Chemistry for Process Metallurgy*. Academic Press, 1997.

[11] P C Hayes. *Process Principles in minerals and materials production*. Hayes, 2003.

[12] T S Kho, D R Swinbourne, and T Lehner. Cobalt distribution during copper matte smelting. *Metallurgical and Materials Transactions*, 37B:209–214, 2006.

[13] A Yazawa. Distribution behavior of various elements in copper smelting systems. *Canadian metallurgical quarterly*, 13:443, 1974.

[14] V Kress. Thermochemistry of sulfide liquids iii: Ni-bearing liquids at 1bar. *Contrib Mineral Petrol*, 154:191–204, 2007.

[15] S Wright, S Jahanshahi, and S Sun. Activities of cu, fe and ni in cu-fe-ni mattes. In *VII International Conference on Molten Slags Fluxes and Salts*, 2004.

[16] E A Brandes and G B Brook, editors. *Smithells Metals Reference Book*. Reed Educational and Professional Publishing Ltd, 1992.

[17] J Nell and J P R de Villiers. T-po2 topologic analysis of phase relations in the system cao-cro-cr2o3-sio2. *Journal of the American Ceramic Society*, 76 no.9:2193 – 2200, 1993.

[18] N Bartie. The effects of temperature, slag chemistry and po2 the behavior of chromium oxide in melter slags. Master's thesis, Stellenbosch University, 2004.

[19] A McKenzie. The solubility of chromium in silicate melts. 1998.

[20] H G Kim and H Y Sohn. Effects of cao, al2o3 and mgo additions on the copper solubility, ferric/ferrous ratio, and minor-element behavior of iron-silicate slags. *Metallurgical and Materials Transactions B*, 29 B:583 – 590, 1998.

[21] J P R de Villiers. Liquidus-solidus phase relations in the system cao-cro-cr2o3-sio2. *Journal of the American Ceramic Society*, 75 no.6:1333 – 1341, 1992.

[22] A Muan and S Sominya. *Journal of the American Ceramic society*, Vol.43 No.10:531–541, 1960.

[23] Verein Deutscher Eisenhuttenleute. *Slag Atlas*. Verlag Stahleisen GMbH, Dusseldorf, 1995.

[24] F Kongoli and A Yazawa. Liquidus surface of feo-fe2o3-sio2-cao slag containing al2o3, mgo and cu2o at intermediate oxygen partial pressures. *Metallurgical and materials transactions B*, 32B:583–592, 2001.

[25] In-Hu Jung, S A Decterov, and A D Pelton. Critical thermodynamic evaluation and optimization of the feo-fe2o3-mgo-sio2 system. *Metallurgical and Materials Transactions B*, 35B:877–889, 2004.

[26] W Ping, G Eriksson, and AD Pelton. Critical evaluation and optimization of the thermodynamic properties and phase diagrams of the cao-feo, cao-mgo, cao-mno, feo-mgo, feo-mno and mgo-mno systems. *Journal of the American Ceramic Society*, 76 [8]:2065 – 2075, 1993.

[27] G Eriksson and A D Pelton. Critical evaluation and optimization of the thermodynamic properties and phase diagrams of the cao-al2o3, al2o3-sio2 and cao-al2o3-sio2 systems. *Metallurgical Transactions B*, 24B:807 – 816, 1993.

[28] A D Pelton and M Blander. Thermodynamic analysis of ordered liquid solutions by a modified quasi-chemical approach - application to silicate sllags. *Metallurgical transactions*, 17B [4]:805 – 815, 1986.

[29] In-Ho Jung, S Dectrovec, and A D Pelton. Thermodynamic modeling of the mgo-al2o3-cro-cr2o3. *The Journal of the American Ceramic Society*, 88[7]:1921–1928, 2005.

[30] P Walder and A D Pelton. Critical thermodynamic assessment and modeling of the fe-ni-s system. *Metallurgical and Materials Transactions B*, 35B:897–907, 2004.

[31] P Vandasz, K Tomasek, and M Havlik. Physical properties of feo-fe2o3-sio2-cao melt systems. *Acrhives of metallurgy*, 46:279–290, 2001.

[32] J L Margrave. *Refractory materials, a series of monographs, department of chemistry.* 1970.

[33] D F Lupton, J Merker, and F Scholz. The correct use of platinum in the xrf laboratory. *X-Ray Spectometry*, 26:132–140, 1997.

[34] M Kwatara. Chromium deportment in copper matte equilibrated with crxo-containing sla chromium deportment in copper matte equilibrated with crxo-containing slag. Master's thesis, Stellenbosch University, 2006.

[35] M D Koretsky. *Engineering and Chemical Thermodynamics.* Wiley, 2004.

[36] W Banda. *High Temperature Phase Equilibria in the Fe-Co-Cu-Si System Pertinent to Slag Cleaning.* PhD thesis, Departmnet of Process Engineering, University of Stellenbsoch, 2006.

[37] S McCullough. Personal communication (email), 2007.

[38] D L Kaiser and Elliot J F. Solubility of oxygen and ssulphur in copper-iron mattes. *Metallurgical Transactions B*, 17B:147–157, 1986.

[39] H E Jamieson and P L Roeder. The distribution of mg and fe2+ between olivine and spinel at 1300oc. *American Mineralogist*, 69:283–291, 1984.